REDUNDANT STRAIN OBSERVATIONS IN SOUTHERN NEVADA: STRAIN STEPS FROM THE HANDLEY NUCLEAR TEST AND SECULAR STRAINS

by

Lawrence H. Kumamoto

A Thesis submitted to the Faculty and the Board of Trustees of the Colorado School of Mines in partial fulfillment of the requirements for the degree of Master of Science in Geophysics.

Signed: Lawrence H. Kuramoto

Golden, Colorado

Date: 22 May, 1973

Approved: Maurice W. Major

Maurice W. Major
Thesis Advisor

Ralph C. Holmer

Ralph C. Holmer
Head, Department of
Geophysical Engineering

Golden, Colorado

Date: May 24, 1973

ABSTRACT

A Colorado School of Mines-Earthquake Mechanisms Lab strainmeter network in southern Nevada has provided data from the Handley underground nuclear test and secular strains in 1970 and 1971. The Handley strain steps were observed at station SCT with 4 horizontal and one vertical component; the least-squares lemniscate fitted to the steps has residuals less than the 5% calibration uncertainty, and a minimum extension axis radial to the source. The Poisson's ratio calculated from areal and vertical strain is 0.45.

Yearly strain changes, 2×10^{-5}, and problems in the determination of Poisson's ratio for the secular data suggest substantial inelastic deformation. Yearly deviatoric strain lemniscates exhibit a correspondence to local tectonic trends, while secular areal strains vary from 2×10^{-5} EXT, to 3×10^{-5} COMP within 50 km. The site specific areal strain introduces a difficulty into the estimation of 'regional' strain fields.

Comparison of Handley steps and the secular strains at SPM and SCT indicates that areal strains at both stations are in the same sense for step and secular data; the deviatoric strain at SPM can be related to the local secular trend as well as to the shot source. A mechanism relating steps and prestress is provided by the non-linear, internal friction model of White (1969a).

CONTENTS

ILLUSTRATIONS

TABLES

ACKNOWLEDGEMENTS

Thanks are extended to Prof. M.W. Major, thesis advisor, and Prof. R.F. Yeatts and Dr. P.R. Romig, committee members. The author gratefully recognizes his indebtedness to Dr. D.L. Butler, Prof. C.J. Wideman, P.L. Brown, and Ms. Cindy Guu.

This work was supported by the National Oceanic and Atmospheric Administration under contracts N 22-19-72(G) and 04-4-022-1.

INTRODUCTION

Since Benioff (1935) first proposed the linear strain seismograph, instruments modelled upon his have been used to study earth strain phenomena ranging from seismic waves to the tides and free modes of the earth. The Nevada strain network operated by the Colorado School of Mines for the Earthquake Mechanisms Laboratory of NOAA has provided a unique opportunity to investigate the behavior of such instruments through the use of redundant measurements. Redundancy, as used here, means the overconstraining of the elastic equations by taking more measurements than are necessary to uniquely specify the state of strain. The network allows redundancy at a point and over an area. Both strain step data from the Handley nuclear test and secular strains will be treated in this manner.

The existence of residual strain steps associated with earthquakes and underground nuclear explosions is well documented, Press and Archambeau (1962), Press (1965). The observation of such steps by means of quartz-tube extensometers has also been documented by Romig, et al, (1969) and Wideman and Major (1967). Doubt as to the actual significance of the instrumentally observed steps has persisted, however, due to the possibility of instrumental hysteresis, non-linearity, local readjustments of irregularly coupled blocks of earth, or local site-specific variations in elastic parameters. The strain steps associated with the Handley underground test and observed at Scotty's Junction, Nevada, permit a crucial test of the randomness of the steps. The problem addressed is the nature of strain steps, whether instrumental or in the ground.

Secular strain measurements have been similarly questioned. The existence of yearly cycles in trenched, quartz-tube strainmeter data has been noted by Romig (1969). Although not all of the data to be presented here spans a full year, the observations exhibit large amplitude seasonal cycles which must be recognized in order to interpret the data. The secular strain measurements at several stations permit the scrutiny of several questions,whether secular strains represent local slump or tectonic effects, whether regional strain fields may be reliably inferred from such data, and whether strain steps induced by transients bear any relation to pre-existing tectonic strains.

INSTRUMENTATION

Since questions of instrument behavior and of near site behavior are to be discussed, it is appropriate to begin by discussing the station sites and the instruments themselves.

The Colorado School of Mines and the Earthquake Mechanisms Laboratory of the National Oceanic and Atmospheric Administration maintained 4 strainmeter stations on the periphery of the Nevada Test Site during 1970. The map locations of these stations are shown in Fig. 1. The Scotty's Junction station, designated SCT, is situated in a fractured, ash-flow tuff overlain by approximately 4 feet of unconsolidated alluvium, on the northern side of Grapevine Canyon. The Sleeping Mountain station, designated SPM, is located on a massive block of welded ash at the base of a cinder cone at the juncture of Pahute Mesa and Sarcobatus Flat. The Thirsty Canyon station, designated TRC, is based on a massive, blocky tuff atop a southward projecting nose of Pahute Mesa. The Twin Springs station, designated TSP, is located on contorted volcanics in a saddle at the southern-most tip of the Pancake Range. The one component station designated ELY and the station

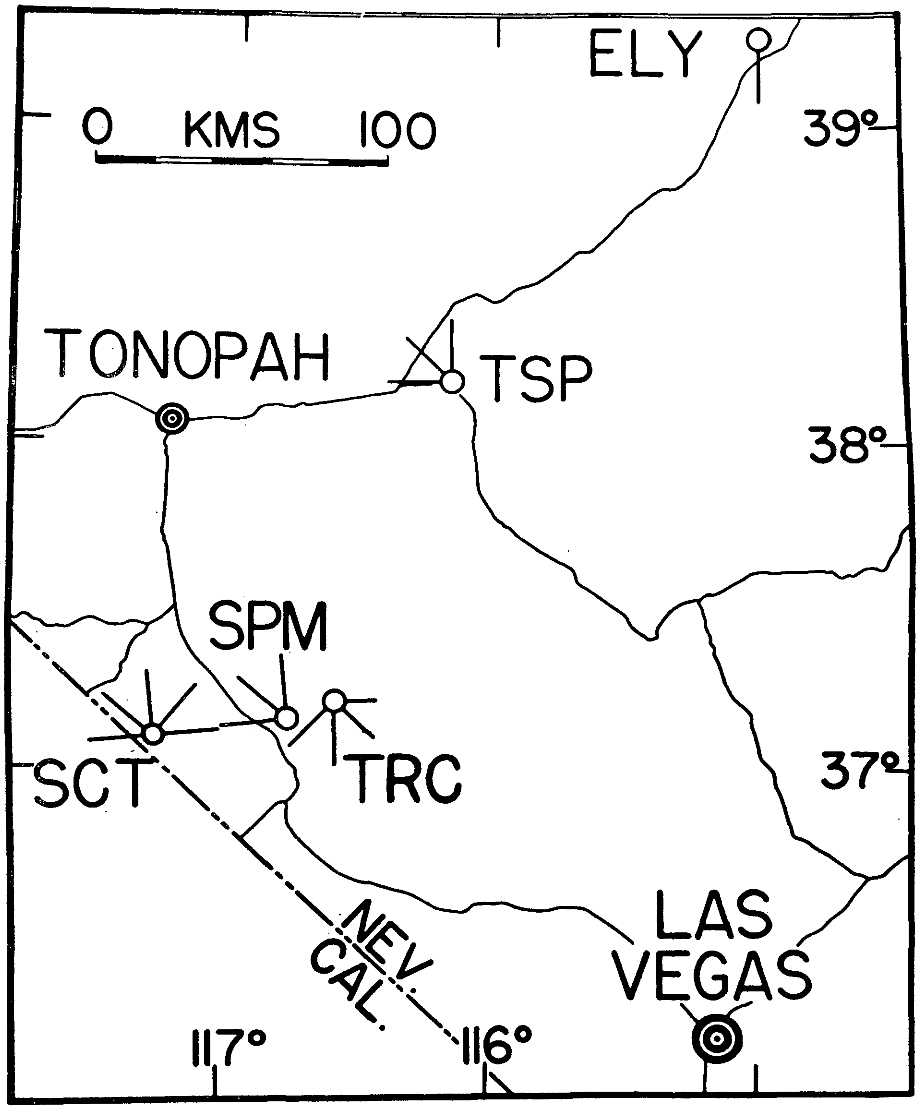

Figure 1. Site map of Nevada station locations.

TABLE 1.

STATION	COORDINATES & ELEVATION	COMPONENT LENGTH	COMPONENT AZIMUTH
THIRSTY CANYON (TRC)	37°12.19' N	19'2"	N46°E
	116°34.70'W	19'2"	N 5°E
	+5440'	19'2"	N40°W
		19'2"	N84°W
SLEEPING MOUNTAIN (SPM)	37°08.6' N	19'2"	N84°E
	116°46.0' W	19'2"	N 6°W
	+4400'	19'2"	N51°W
SCOTTY'S JUNCTION (SCT#1)	37°05.5' N	29'2"	N84°E
	117°16.05'W		
	+4320'		
SCOTTY'S JUNCTION (SCT#2)	37°05.34' N	39'2"	N84°E
	117°16.27'W	39'2"	S 6°E
	+4280'	39'2"	S39°W
		39'2"	N51°W
		24'2"	VERTICAL

designated TSP have not provided sufficient data for interpretation and will not be discussed in this paper.

The instruments are quartz-tube extensometers of the Benioff design (Benioff, 1959) with modified capacitive displacement transducers and integral micrometer calibration (Romig, 1967). Quartz-tube length standards are suspended by wire in 5-inch jacket-pipe and one end embedded in a concrete pier. At the other end, the jacket-pipe is bolted to a second pier and the quartz allowed to hang freely. A displacement transducer is fixed to the free-end pier and senses movement of the quartz with respect to the free-end pier. The free-end is encased in a timber endhouse with surface access. The trenches, ranging from 3- to 5-feet deep, are backfilled and compacted. Access hatchways are insulated with rubber seals and styrofoam plugs. Temperature compensation is effected by means of aluminum fold joints between adjacent 10-foot sections of quartz rod. The temperature noise from the tube and air gap has been estimated by Romig (1967) as less than 1×10^{-7} per degree Centigrade. Temperature effects on the metal components of the transducer and mounting plates are not, as yet, well determined, but they are suspected to comprise the major portion of the observed noise. Site parameter are detailed in Table 1.

As is seen from Table 1, the SCT station consists of two separate sites. SCT #1, the original site constructed to measure strains resulting from the Benham nuclear test, consists of a single component which was eventually abandoned as it became apparent that it was situated in the local drainage pattern.

SCT #2, less than half a mile west of SCT #1, contains four horizontal components, one of which is oriented in the same direction as SCT #1, and a vertical strainmeter within 50 feet of the main station. The four horizontal components share a common free-end pier and endhouse. The construction of the vertical component, Fig. 2, differs from that of the others in that a single section of quarts, 25 feet in length, was grouted to the bottom of a cased hole. Since the single section of quarts is not temperature compensated, special care was taken to bury and insulate the endhouse. This vertical strainmeter is unique in the literature in that it is situated at the surface of the earth.

At TRC, which also has four horizontal components, all components share a common free-end pier, wheras at SPM, each component is separate.

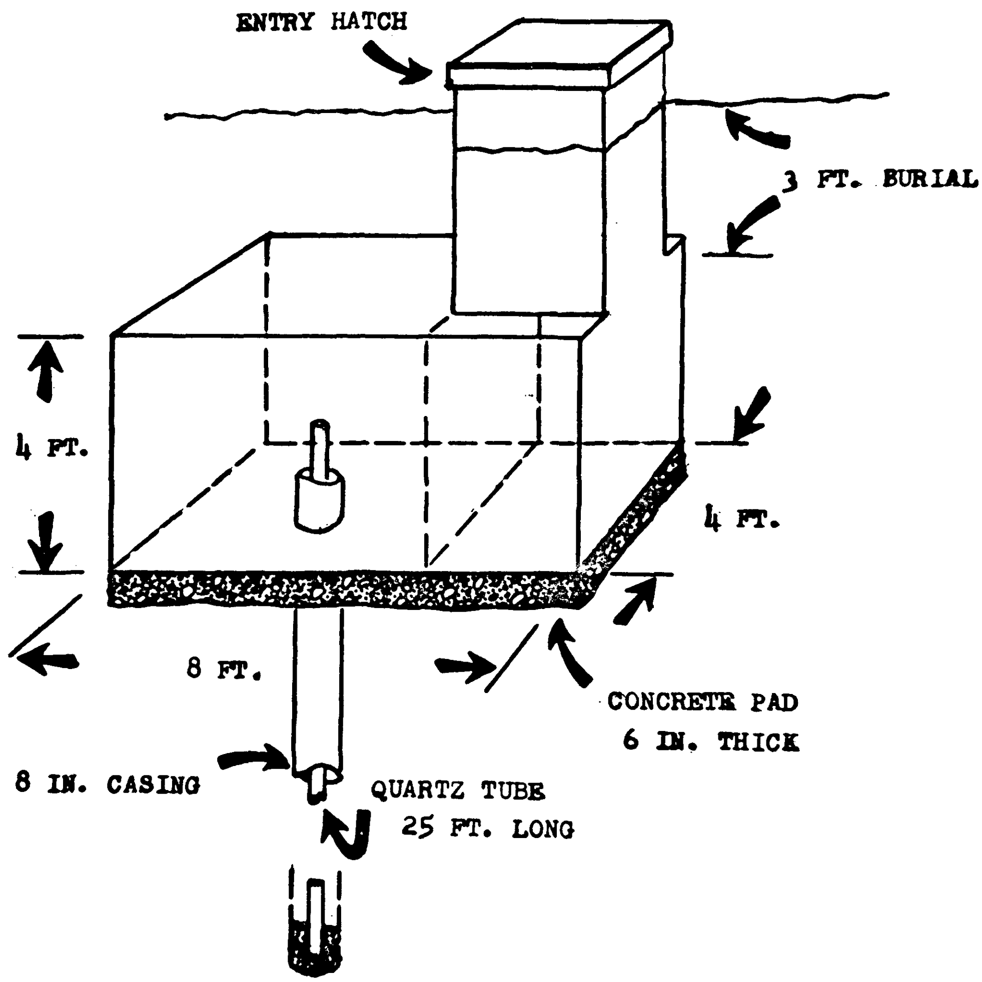

Figure 2. Schematic of SCT vertical strainmeter.

THEORY OF STRAIN MEASUREMENTS

As the behavior of the earth is to be inferred by measuring the relative displacement between two points some tens of feet apart, it is appropriate that the assumptions of strain theory be discussed first. The concepts of infinitesimal strain measured by finite length strainmeters, of the invariance of areal strain, and of the relationship between vertical strain and areal strain at a free surface are treated in this section.

A state of relative strain is specified by the gradient of a displacement field. The general Eulerian strain components (Sokolnikoff, 1956, p. 30) are given by:

$$E_{ij} = \frac{1}{2} \left(u_{i,j} + u_{j,i} - u_{i,j}u_{j,i} \right) \tag{1}$$

where $u_i = u_i(x^1, x^2, x^3)$, the displacement vector field, and x^i are orthogonal Cartesian space co-ordinates, and the comma indicates covariant differentiation. This casting of strain is non-linear and non-superposable. For $u_{i,j}$ much less than 1, the second order term, $u_{i,j}u_{j,i}$ may be disregarded as negligible and the infinitesimal strain tensor,

$$e_{ij} = \frac{1}{2} (u_{i,j} + u_{j,i}) \tag{2}$$

is obtained. Infinitesimal strain is linear and superposable.

The earth strains observed near the surface, over time intervals of seconds to years, range from 1×10^{-8} for the earth tides, to nearly 1×10^{-4}, the breaking strain of rocks at the surface. In such cases, the second order term, $u_{i,j}\, u_{j,i}$, ranges from 1×10^{-8} to 1×10^{-16}, well outside the range of consideration of finite strain.

Rotation, as well as strain, is determined by the gradient of the displacement field, and the rotation tensor w_{ij} is given by

$$w_{ij} = \frac{1}{2} (u_{i,j} - u_{j,i}) \tag{3}$$

Since rotations are not detectable with extensometers, it is assumed that they are of the same order of magnitude as the strains, so that instrument azimuths, known to within $.5^{\circ}$, are uneffected by

$$w_{ij} \approx 10^{-4} \approx .01^{\circ} - .001^{\circ}$$

With this assumption and the infinitesimal nature of the strain, the instruments are considered to maintain a constant azimuthal orientation, and orthogonal Cartesian co-ordinate axes coinciding with instrument axes are adopted.

The only restriction thus far are the equations of compatibility (Sokolnikoff, 1956, p. 25-28),

$$e_{ij,kl} + e_{kl,ij} - e_{ik,jl} - e_{jl,ik} = 0 \qquad (4)$$

which ensure the continuity and single-valuedness of the displacement field. These space derivatives of strain are not detectable with existing arrays of instruments, but it must be assumed that over the physical point of measurement, the displacement field has no discontinuities or that they are so small and so numerous that they are averaged out. This assumes the medium to be physically continuous over the "point" of measurement.

The instrument described in the previous section is a relative displacement meter. The output "strain" is the change in length of the baseline, divided by the length of the quartz-bar standard, or:

$$e_{11} = \frac{1}{L} \left(u_1(+L/2, x^2) - u_1(-L/2, x^2) \right) \qquad (5)$$

where $x^1 = 0$ at the midpoint of the strainmeter and the x^1-axis is parallel to the baseline.

Consider the strainmeter of finite length L as a linear differentiation operator acting on the displacement field such that:

$$e_{11}(0) = \frac{1}{L}\left(\delta(x^1 - \frac{L}{2}) - \delta(x^1 + \frac{L}{2}) \right) u_1(x^1, x^2) \tag{6}$$

The spatial frequency or wave number characteristic of this approximate operator is determined as:

$$F_L(k^1) = \frac{1}{L}\,(e^{i\frac{L}{2}k^1} - e^{-i\frac{L}{2}k^1}) = \frac{2i}{L} \sin(\frac{L}{2}\, k^1) \tag{7}$$

where k^1 is the spatial frequency in the x^1 direction. Separating this into modulus, $A_L(k^1)$, and phase, $\Phi_L(k^1)$, we have

$$A_L(k^1) = \frac{2}{L} \left| \sin(\frac{L}{2}\, k^1) \right|$$

$$\Phi_L(k^1) = \frac{\pi}{2} \text{ signum } (\sin(\frac{L}{2}\, k^1)) \tag{8}$$

The ideal "point" strainmeter located at $x^1 = 0$ will yield

$$e_{11}(0) = \frac{\partial u_1}{\partial x_1} = \delta(x^1)\, u_1(x^1, x^2) \tag{9}$$

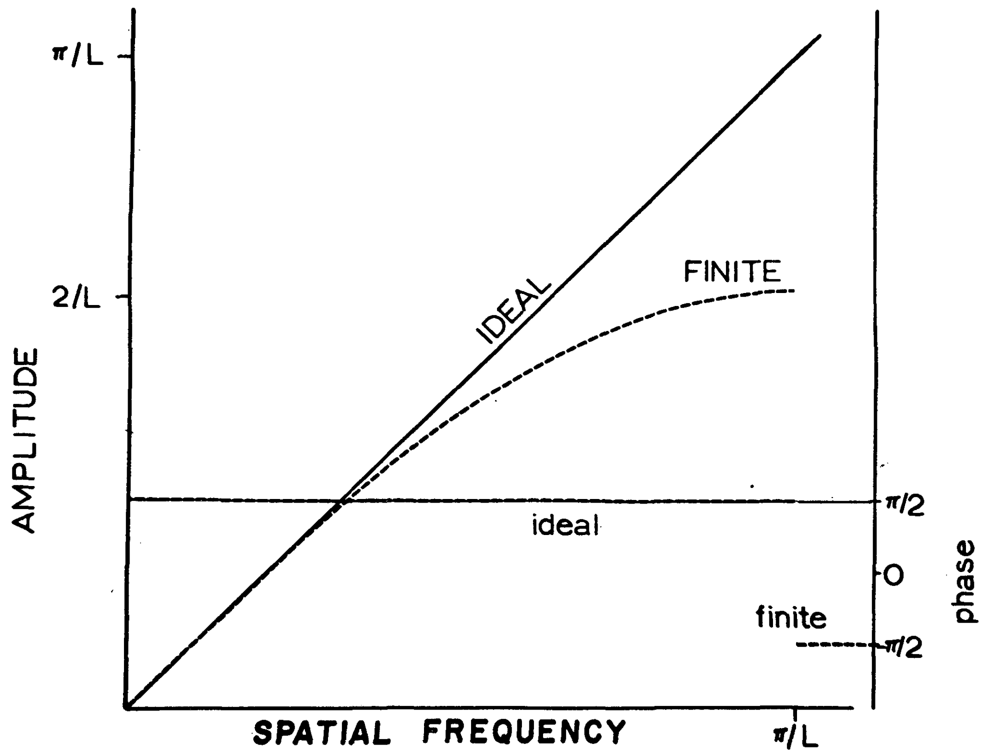

Figure 3. Strainmeter spatial frequency response.

so that

$$F(k^1) = ik^1 \tag{10}$$

$$A(k^1) = \left| k^1 \right| \tag{11}$$

and,

$$\Phi(k^1) = \frac{\pi}{2} \text{ signum } (k^1) \tag{12}$$

The modulus and phase of both the "perfect" strainmeter and the strainmeter of finite length L are plotted in Fig. 3. For $k^1 < \frac{2\pi}{100L}$, the phases are identical and modulus is reasonably undistorted. The spatial frequencies of seismic disturbances are well below the upper bound for 50-foot-long instruments.

The problem has been reduced to infinitesimal, point strain and the classical theory is applicable. From the conventions of tensor calculus, the transformation of a tensor from one co-ordinate system to another is by,

$$e_{mn}(z) = \frac{\partial x^i}{\partial z^m} \frac{\partial x^j}{\partial z^n} e_{ij}(x) \tag{13}$$

where z^i are the co-ordinates of the transformed system.

At a stress-free surface with the x^3 axis normal to the surface, e_{33} is a principal strain and the other two are tangent to the surface. For this case, considering rotations of axes about the normal, the transformation is,

$$\begin{Bmatrix} x^1 \\ x^2 \end{Bmatrix} = \begin{Bmatrix} \cos\phi, & -\sin\phi \\ \sin\phi, & \cos\phi \end{Bmatrix} \begin{Bmatrix} z^1 \\ z^2 \end{Bmatrix} \tag{14}$$

so that,

$$e_{11}(z) = e_{11}(x)\cos^2\phi + e_{22}(x)\sin^2\phi + 2e_{12}(x)\sin\phi\cos\phi$$

$$e_{22}(z) = e_{11}(x)\sin^2\phi + e_{22}(x)\cos^2\phi - 2e_{12}(x)\sin\phi\cos\phi$$

$$e_{12}(z) = \left(e_{22}(x) - e_{11}(x)\right)\sin\phi\cos\phi + e_{12}(x)\left(\cos^2\phi - \sin^2\phi\right) \tag{15}$$

For the standard Nevada array, with 2 orthogonal components and another at 45 degrees between them, the instruments are used as axes and e_{11} and e_{22} are measured directly and e_{12} is determined from,

$$e_{12} = e(45^\circ) - \frac{1}{2}\,(\,e_{11} + e_{22}\,) \tag{16}$$

The resulting strain tensor is diagonalized in optimum co-ordinates according to:

$$(e_{ij} - E\,\delta_{ij}\,)\,A_j = 0 \quad \text{(Sokolnikoff, 1956, p. 16)}, \tag{17}$$

where the eigenvalues, the 3 values of E, are the principal strains, and the eigenvectors, A_j, are unit vectors whose components are the direction cosines of the optimum co-ordinate axes.

The first test of consistency is based on the invariance of the areal strain, the sum of the strains in any 2 orthogonal directions in the plane. It is readily observable from the equations of transformation, eqns. (15), that the sum of e_{11} and e_{22} in any co-ordinate system rotated in the plane will be equal,

$$e_{11}(z) + e_{22}(z) = e_{11}(x) + e_{22}(x) \tag{18}$$

A second test of the consistency of the strain measurements involves the following assumptions. It is assumed that the instruments are located at a stress-free surface. This condition has been shown valid at depths of several hundred meters for seismic events and earth tides, (Major, et al, 1964). The furthur assumptions of a Hookean stress-strain relationship and homogeneity and isotropy over the physical point of measurement permit,

$$p_{ij} = \lambda(e_{11} + e_{22} + e_{33})\,\delta_{ij} + 2\mu e_{ij} \tag{19}$$

and,

$$p_{33} = 0 = \lambda(e_{11} + e_{22}) + (\lambda + 2\mu)\, e_{33} \tag{20}$$

or,

$$e_{33} = -\frac{\lambda}{\lambda + 2\mu}(e_{11} + e_{22}) \tag{21}$$

The vertical strain is proportional to the areal strain. A vertical strain measurement in conjunction with an areal strain measurement permits a determination of the $\frac{\lambda}{\mu}$ ratio, and Poisson's ratio,

$$\sigma = \frac{\lambda}{2(\lambda + \mu)} \tag{22}$$

The physical plausibility of the computed Poisson's ratio and its fit to other measured values provides a measure of the "idealness" of the instruments and the ground.

The presence of 4 horizontal strainmeters at SCT permits the test of invariance for areal strain, and the vertical strainmeter allows a Poisson's ratio to be computed.

THE HANDLEY EVENT

The Handley nuclear test, 1900GMT, 16 March 1970, was monitored at all 4 stations, however, TRC, the closest of them to shot, 12.5 km, underwent large accelerations. There, total movement on several components was not determined because the capacitor plates bounced together. The strain steps from all the sites have been reported by Yeatts (1970). The only station which allowed redundant measurement was SCT which registered steps on all components. It is the SCT data that is discussed in the following development.

The SCT #2 data plots are shown in Fig. 4. The strain change residuals used are the 5-minute static steps, that is, the difference between pre-shot reference levels and the levels 5 minutes after the first arrival. Instrument thermal drift, due to open endhouse hatches, was removed by straight line extrapolation of pre-shot drift. The thermal effects were particularly high on the NW component record because a 10-foot section of aluminum had been inserted in place of a broken section of quartz. Recorder zero-level changes and micrometer adjustments have been removed. Calibrations were determined by plotting one

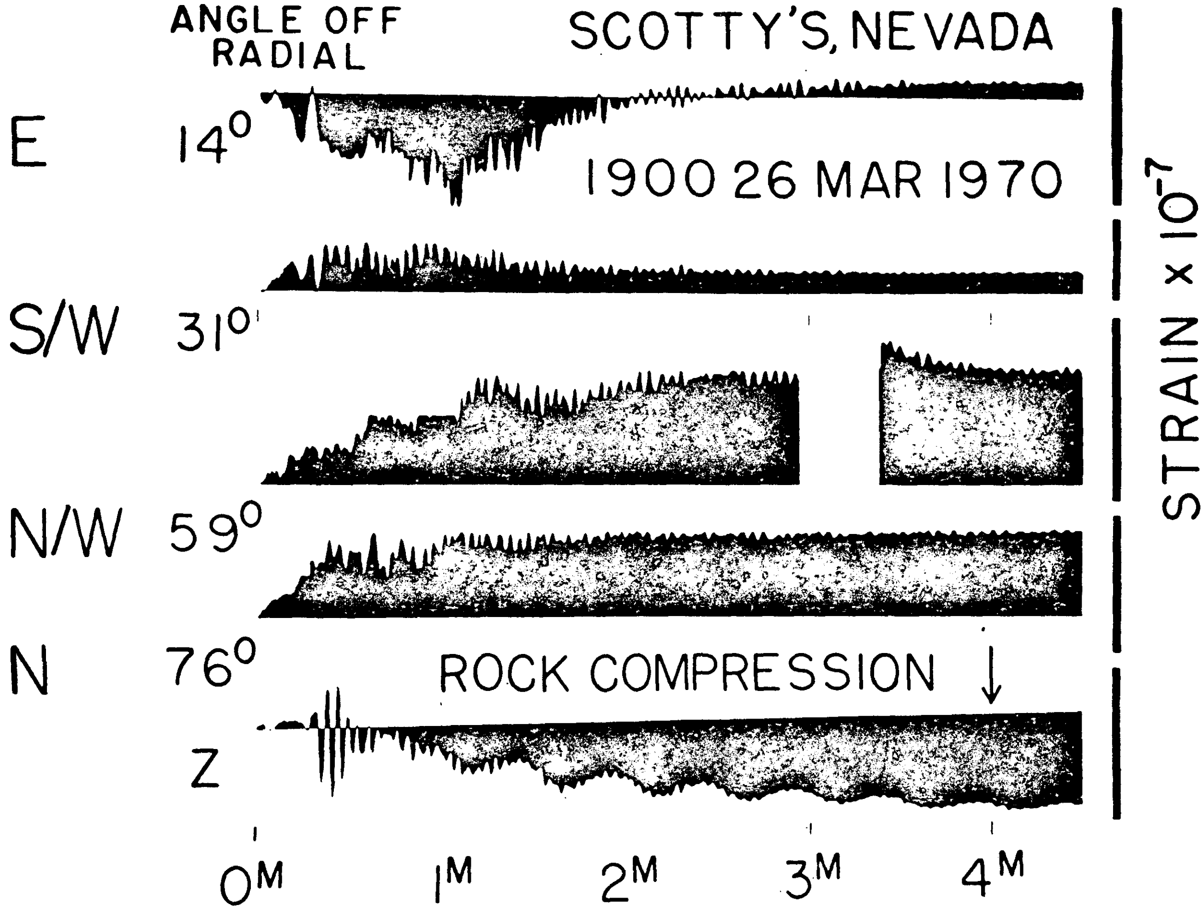

Figure 4. Handley strain records from SCT.

complete revolution of the micrometer, 250-micro-inches, against the total number of chart divisions of deflection. Note that the calibration bars at the right in Fig. 2 are not the same size. The 30-second oscillation in the dynamic portion of the vertical, or Z, record is one of several dynamic features of the records which are not currently understood. With the exception of the direct comparison of SCT #1 E/W with SCT #2 E/W, only the residual strain steps will be treated in this presentation.

The direct comparison of the SCT #2 E/W and the single E/W component of SCT #1 is shown in Fig. 5. The upper trace is the SCT #2 record, and the area between the 2 traces is blacked in. The similarity is striking for the first 70 seconds, after which time the traces diverge, SCT #2 trace changing sense and going into extension, while the SCT #1 trace goes offscale in compression. The sense of the SCT #1 step is inconsistent with the independent measure of areal strain as will be evident from examination of the azimuthal strain function calculated without SCT #2 E/W in Fig. 6. Note also the loss of sensitivity in the dynamic portion of the record. Although no hard evidence to discount the SCT #1 step has been found, the fact that it did correspond for 70 seconds and then went offscale, while the other remained on the more reliable, near null,

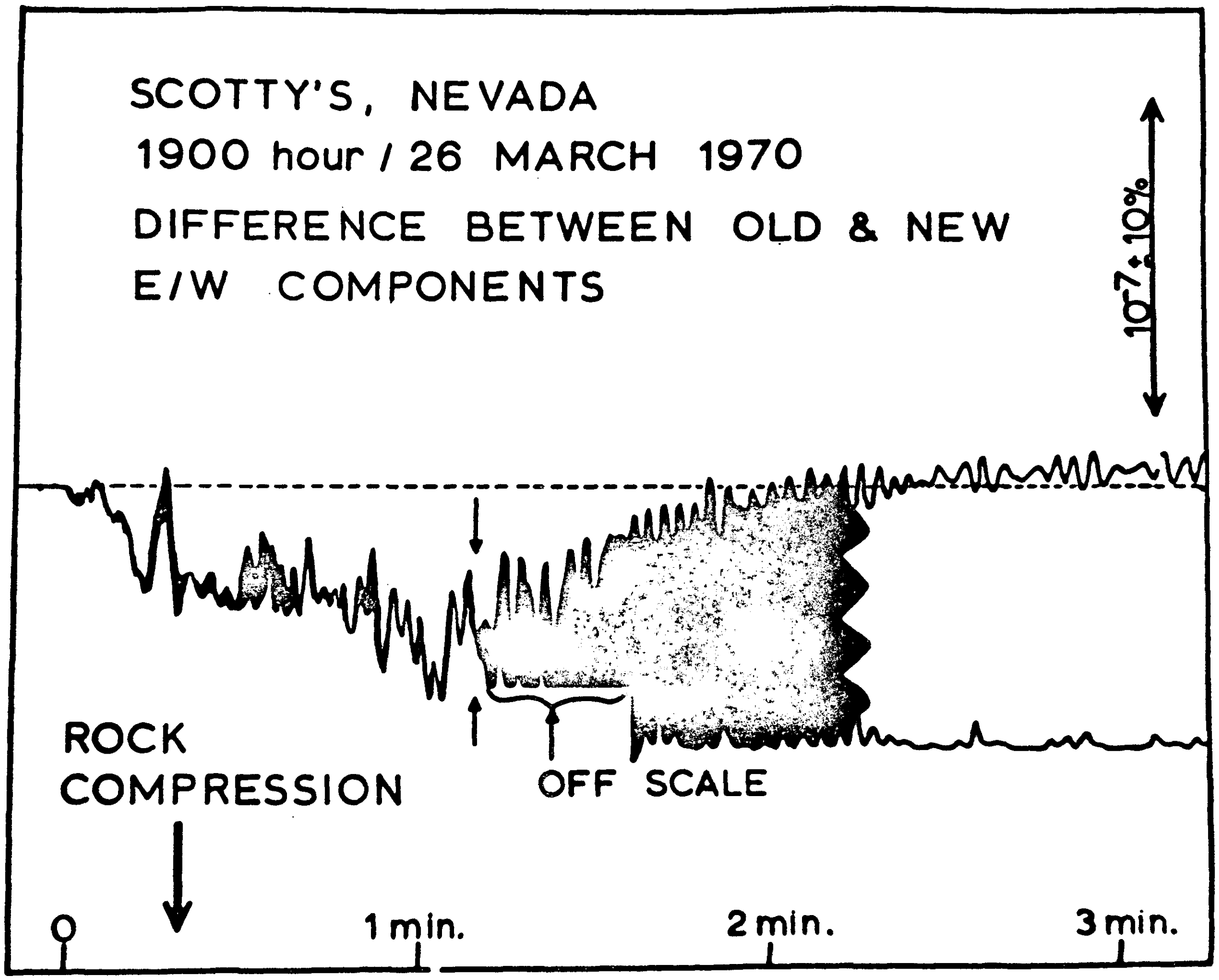

Figure 5. Comparison of E/W #1 and E/W #2 at SCT.

part of the chart, is sufficient to cast doubt upon it.

Table 2 lists the data from SCT #2; no step was picked at SCT #1 because of suspected instrument problems as has been previously discussed. The first column of Table 2 indicates the appropriate component, and the second the measured strain step.

In the third column we have, for each horizontal component, the steps computed from the strain tensor specified by the other three horizontal components. The differences between the measured steps and the computed steps are shown in column 4. Note the repetition and the symmetry of the difference, 1.4×10^{-8}, which is also the difference between the two measured areal strains, that is,

$$1.4 \times 10^{-8} = (e_{N/S} + e_{E/W}) - (e_{NW} + e_{SW}) \neq 0, \text{ or,}$$

$$1.4 \times 10^{-8} = \left| e(\text{computed}) - e(\text{measured}) \right| \qquad (23)$$

The fifth column expresses these strain differences as percentages of their respective recording charts, that is, in chart scale divisions. The strain values for full scale deflection on each instrument are given in column 6. These last two columns are included in order to indicate the size of the differences that would be seen on chart paper, that is, since the difference might be attributed to

TABLE 2. A

HANDLEY EVENT SCT STRAIN STEPS*

COMPONENT	MEASURED STEP	COMPUTED STEP	DIFF.	%F.S. DIFF.	FULL SCALE CALIBRATION
N/S	6.1 EXT	7.5 EXT	+1.4	13%	11.0
NW/SE	5.5 EXT	4.1 EXT	-1.4	17%	8.3
E/W	0.7 EXT	2.1 EXT	+1.4	19%	7.5
NE/SW	2.7 EXT	1.3 EXT	-1.4	7%	19.0
Z	6.0 COMP				10.0

* STRAIN VALUES ARE IN UNITS OF 10^{-8}

TABLE 2. B

MEASURED STRAIN VS. LEAST SQUARE STRAIN*

COMPONENT	MEASURED STEP	LEAST SQ. STEP	RESIDUAL	RESIDUAL % F.S.
N/S	6.1 EXT	6.4 EXT	-0.3	3%
NW/SE	5.5 EXT	5.3 EXT	0.2	2%
E/W	0.7 EXT	0.8 EXT	-0.1	1%
NE/SW	2.7 EXT	2.0 EXT	0.7	4%

any one, or partitioned among any combination of components, a feeling for the sensitivities is necessary. Yet before determining a mean or a least squares fit, another presentation of these differences is necessary.

A quantitative display of the strain tensors may be made by plotting the magnitude of the strains as a polar function of azimuth, that is once having reduced the problem to principal strains and their directions by eqns. (17), and noting that in the optimum co-ordinates the shear strain components are zero, one may use eqns. (15) and obtain,

$$e(\theta) = E_1 \cos^2(\theta - \psi) + E_2 \sin^2(\theta - \psi) \qquad (24)$$

where E_i are the principal strains, and ψ the azimuth of the maximum principal strain axis with respect to a fixed reference axis. It is, in effect, the superposition of the scaled responses of two strainmeters oriented along the axes of the principal strains. The sense of the strain in any direction may be indicated by labeling each lobe as positive or negative. The appeal of this representation rests in the fact that the radial distance from the origin of the polar co-ordinates to the any point on the curve is the magnitude of the strain in the direction of the chosen point. Such figures will be used in this paper and will be referred to as "lemniscates."

Each of the four possible combinations of three measured strain steps specifies a plane strain tensor. Azimuthal strain functions or lemniscates are plotted for each of these combinations in Fig. 6 . All four measured strain steps are plotted as dots with each lemniscate, the three which fall on the curve indicating those steps used to compute the curve. The intersection of the radius drawn to the fourth dot and the curve itself is the computed strain step. The lobes are positive or extensional in all cases except for the combination which excluded the N/E strain step, for which case there are very small negative lobes which are not apparent because of the scale of the lemniscate.

The rather notable qualitative agreement between the four lemniscates is readily apparent, that is, if any one of the instruments had not been operating the remaining three would not have grossly misrepresented the strain field. The axial orientations of the four lemniscates fall within a range of 12° and the differences between magnitudes of semi-major axes are reasonable.

In order to quantify the degree of the fit, a least squares fit has been made. Since the standard least squares procedure weights each reading equally and least squaring

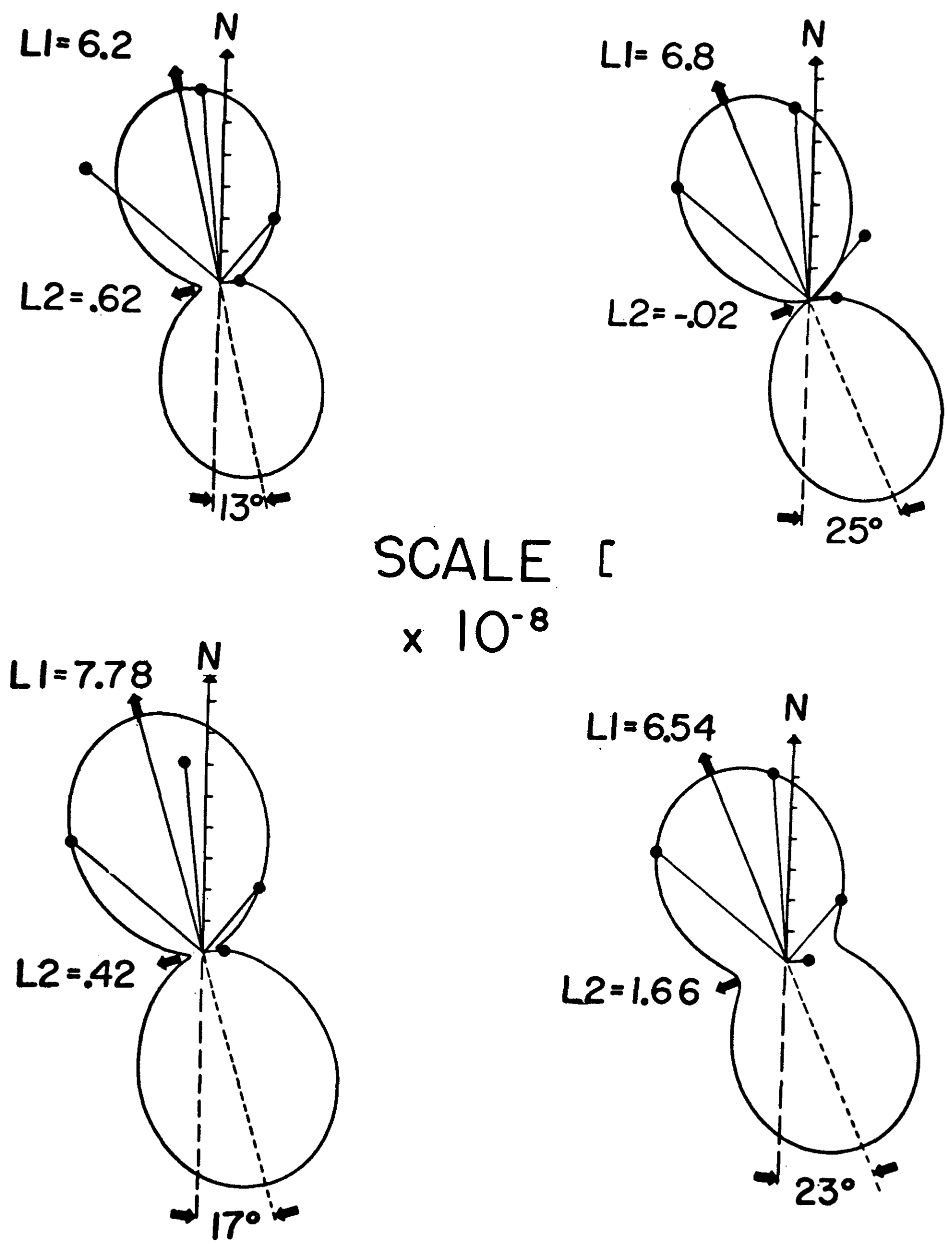

Figure 6. Handley strain lemniscates: computed from groups of three components at SCT.

the percentage of reading residuals weights the smaller readings more heavily, both of these schemes are rejected. It is preferred to weight according to sensitivity and to minimize,

$$\sum_{i=1}^{4} \left(\frac{f_i - e_i}{c_i} \right)^2, \qquad \begin{array}{l} f_i = \text{measured strains} \\ e_i = \epsilon_{11}\cos^2\theta_i + \epsilon_{22}\sin^2\theta_i \\ \qquad +2\,\epsilon_{12}\sin\theta_i\cos\theta_i \end{array} \tag{25}$$

where c_i is the full scale calibration number for the ith reading (from Table 2A). The sum of the squares of the chart scale division differences between observed and best fit values is minimized. The resulting best fit strain tensor is an internally consistent system such that the differences between observed and best fit strains are, in every case, less than 5 scale divisions (Table 2B). Fig. 7, the azimuthal strain function of the best fit strain tensor with the observed strains plotted as dots, indicates an axis of symmetry, the minimum extensional strain axis, 2 degrees from radial to the source. The errors shown by this analysis are well within the recording and calibration uncertainties of the data.

Using the areal strain of the least-squared tensor, 7.2×10^{-8}, and the vertical strain step, -6.0×10^{-8}, the stress-free surface boundary condition, isostropy and homogeneity, we have,

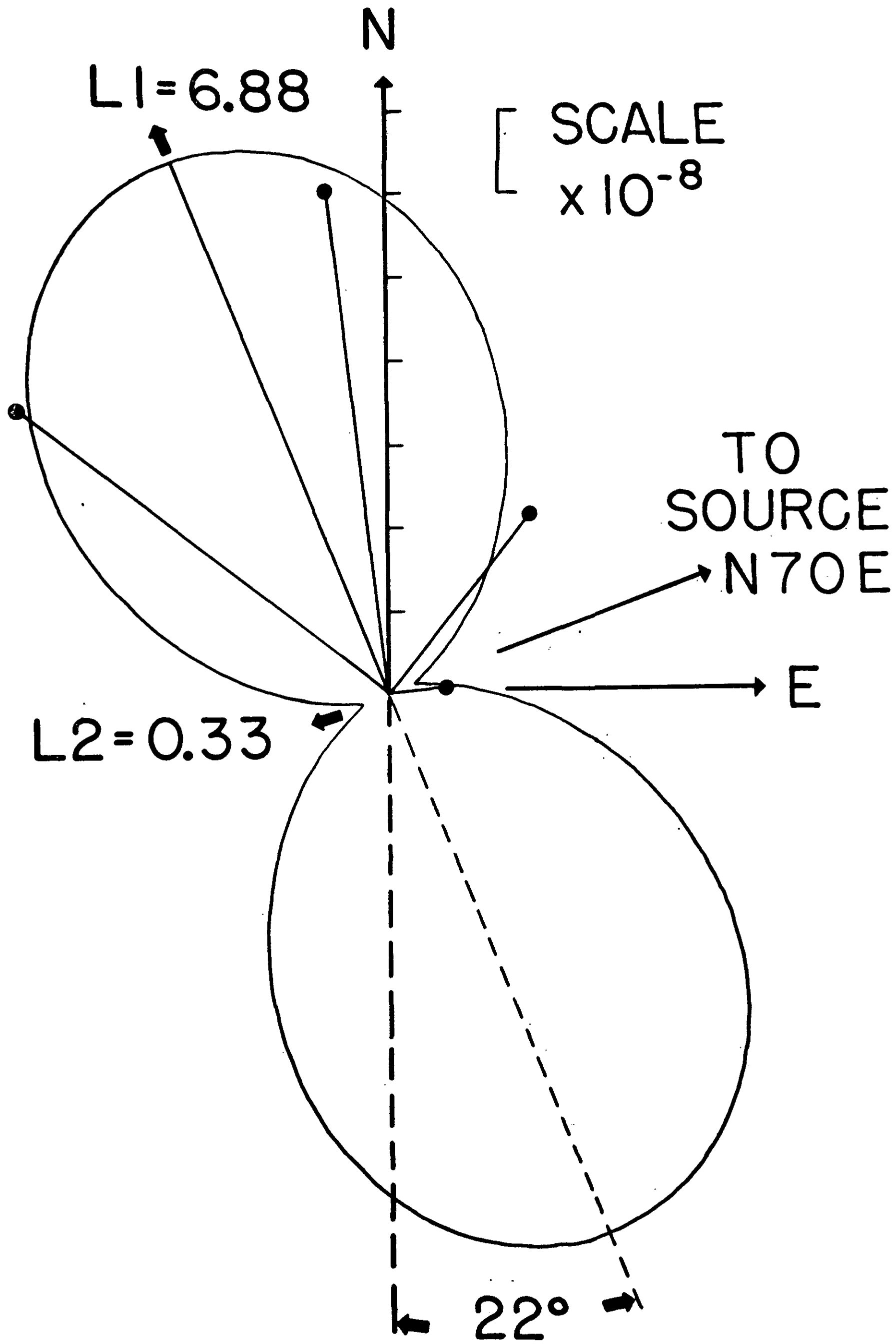

Figure 7. Least square lemniscate from SCT.

$$\frac{\lambda}{\mu} = 9.85, \text{ from eq. 21, and}$$

$$\sigma = 0.45, \text{ from eq. 22.}$$

Yacoub, et al, (1968), determined a Poisson's ratio of 0.405 for the surface layer of 'alluvium and vitric bedded tuff' in their seismic model of a Las Vegas to Pahute Mesa line. Table 3 is a comparison of the SCT elastic constant determination with those of different rock types.

As the possibility of 4 random strain steps yeilding a consistent system is slight, and the chance that when combined with a random vertical strain step they would result in a physically realizable Poisson's ratio is lesser still, it is concluded that the observed steps are true measures of ground deformation and not instrumental eccentricities. The fact that the Poisson's ratio is not only realizable, but also of the order of an independent determination, permits the conclusion that the assumptions of isotropy, elasticity, and the stress-free boundary are well founded. Reference here and subsequent furthur reference to Poisson's ratio is not intended to characterise the site rock but only to indicate the degree of internal consistency of the data. Poisson's ratio is a much used but poor indicator of rock type.

The results indicate no significant deviation from ideal elastic behavior at the point of measurement.

TABLE 3

COMPARISON OF ELASTIC CONSTSNTS

ROCK TYPE	POISSON'S RATIO
QUINCY GRANITE*	.33
PIERRE SHALE**	.43
SCOTTY'S SITE	.45
EAGLE FORD SHALE***	.46- .48

* FROM BIRCH (1942), TABLE 5-13, ELASTICITY OF ROCKS FROM SEISMIC DETERMINATIONS, p. 86.

**FROM WHITE (1965), TABLE 3-1, p. 89, (DETERMINED FROM SEISMIC VELOCITIES OF BULK MEDIUM)

***FROM WHITE (1953), TABLE 1, p. 61, (DETERMINED FROM HORIZONTAL COMPRESSIONAL WAVE SPEED AND SH AND SV SHEAR WAVE SPEEDS)

SECULAR STRAIN IN SOUTHERN NEVADA

This section is divided into two parts, the first of which presents the data from all three sites, TRC, SPM, and SCT, and treats certain common characteristics; the second contains a site by site data analysis. This separation is necessitated by the presence in each record of a cyclic phenomenon which should be discussed before analysing the data.

I THE DATA AND YEARLY CYCLES

Cumulative strain change has been determined for three stations of the CSM-EML Nevada network. Plots of daily micrometer readings were scaled to strain in Figs. 8 to 10. Where recording was discontinuous, the null balance positions observed during maintenance visits at two week intervals were plotted and interpolated between by straight line approximations (broken lines in the figures). Continuity losses (indicated by blanks) were smoothed by slope matching. No other processing was performed upon the data. The data from October 1970 to June 1971 was reduced from data provided by Murdock (1971).

Immediately obvious (especially on the SCT plots) are

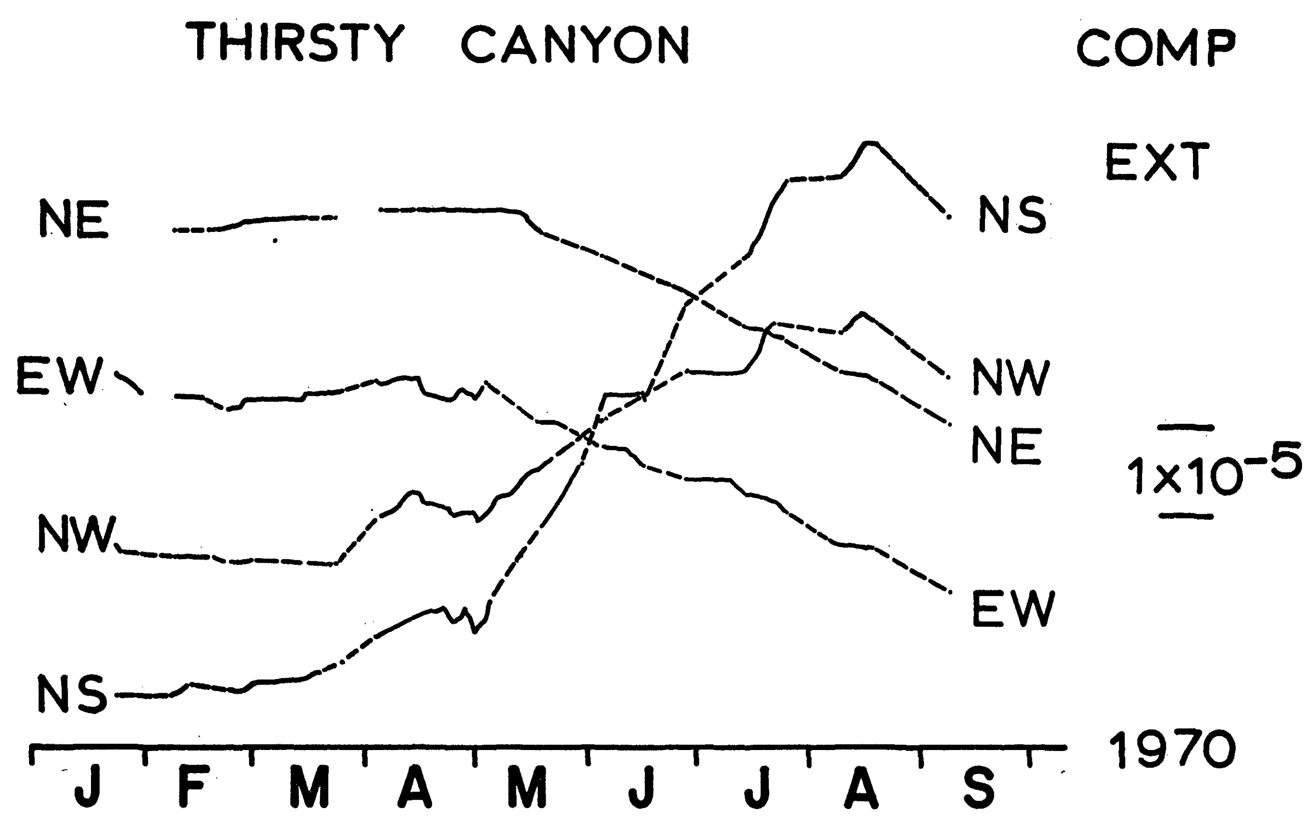

Figure 8. TRC secular data plot: Rock compression up.

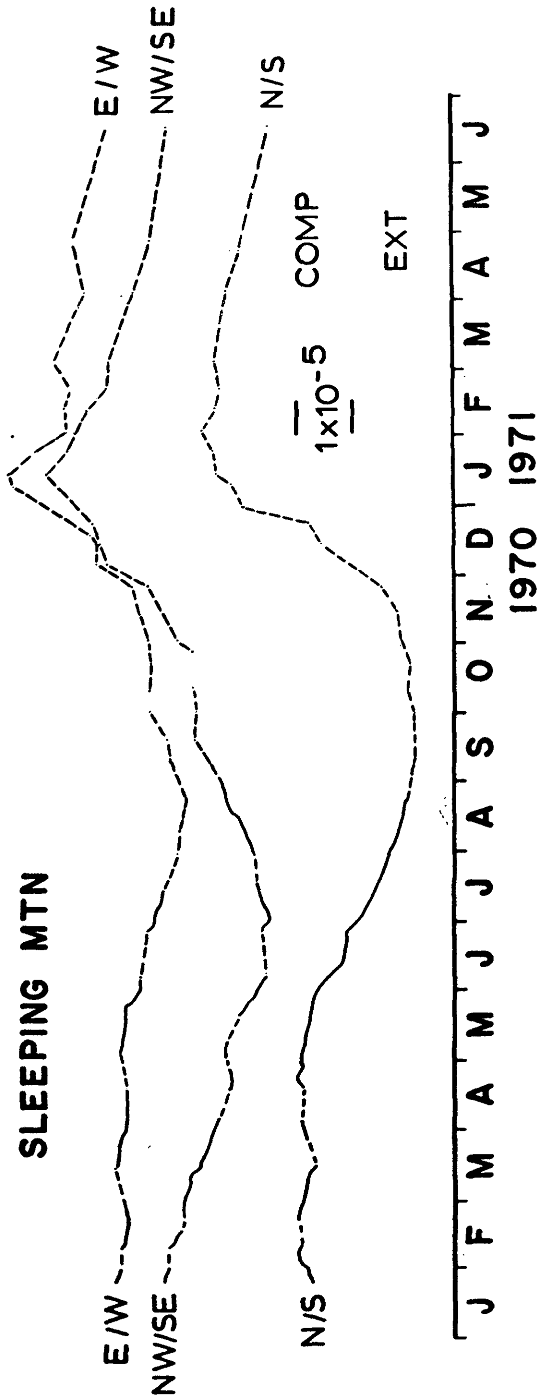

Figure 9. SPM secular data plot: Rock compression up.

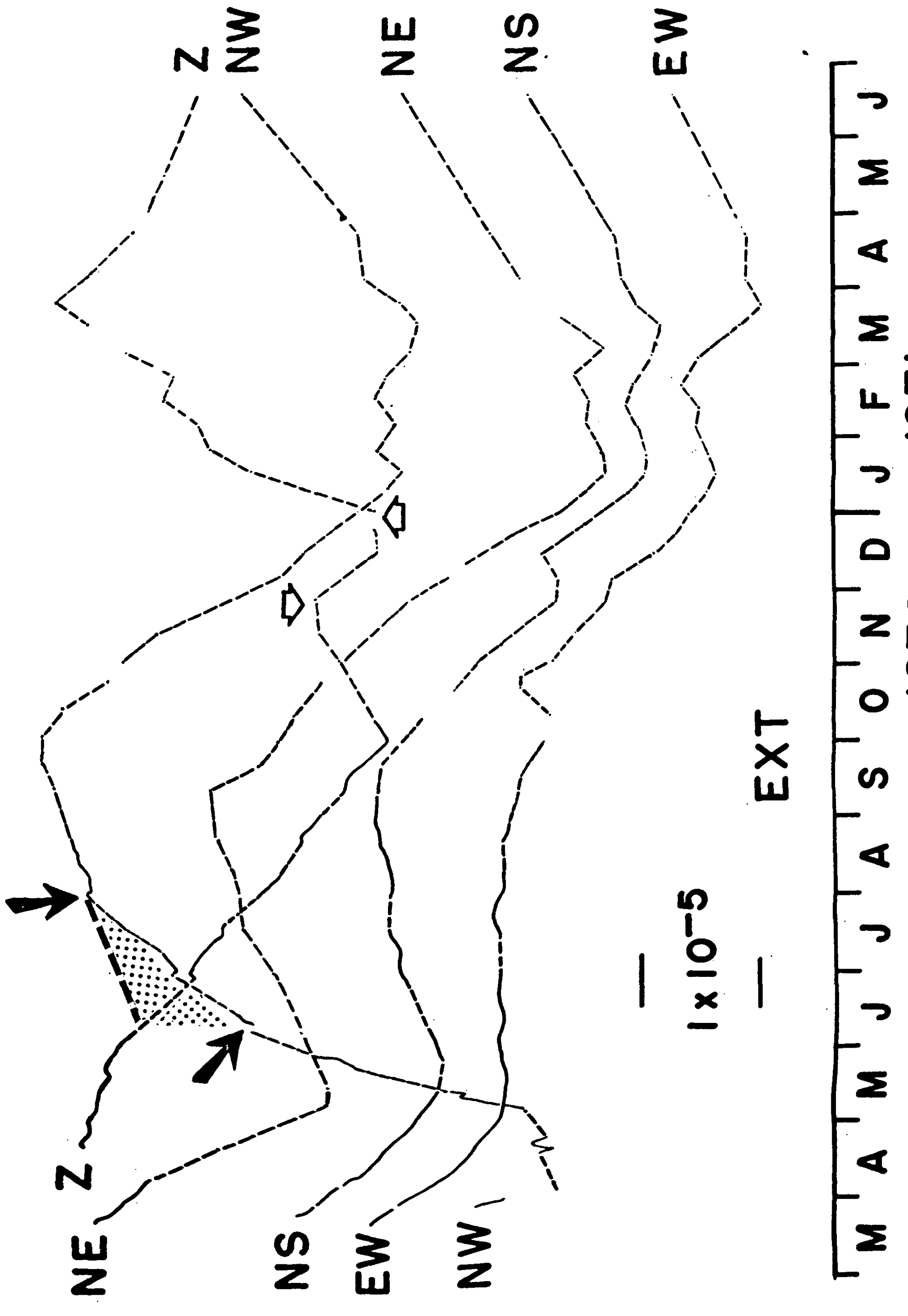

Figure 10. SCT secular data plot: Rock compression up.

the large amplitude quasi-sinusoidal variations. Large scale yearly variations of this type have been previously observed by several authors. Romig (1969), utilizing a two year data string from quartz-tube strainmeters in Northeast Denver, identified the effect as a yearly period seasonal variation and perhaps true earth strains. The existence of such 12-month periodic phenomena has been well accepted, yet the question of whether they represent instrumental or earthstrain effects has remained unanswered. Considering the scale of the Nevada cycles, this question bears directly on the validity of geodetic strain determinations. Cook (1971) using almost three years of data from strainmeters of CSM design in Granite Mountain, Utah, has observed yearly cycles with half amplitudes of 1×10^{-6}. In as much as the Granite Mountain vaults are situated deep within tunnels in a controlled temperature environment, the effect is, perhaps, not purely instrumental. Berger (1972) investigating two years of data from the UCSD-NSF laser strainmeter at Pinon Flat, California, has observed a yearly cycle of half amplitude 5×10^{-7}. Since the laser path is well protected from environmental effects by vacuum pumping this is assumed to be earthstrain. Brown (1972) made observations of strain rates with a quartz-tube strainmeter adjacent to Berger's instrument and reports rates 40 times greater than those observed with the laser, however, Ryall (1972) sees no cycles at all in the mine-shaft of Round Mountain, Nevada.

More recently, both Wideman (personal communication), and Brown (thesis in preparation) have identified similar cyclic phenomena observed in the Aleutian Islands (with trenched strainmeters of CSM design) as related to thermal effects on the metal components of the mechanical transducers. They have shown that by reversing the orientation of the micrometer mounting the cycle is changed in phase by 180°. The exact phase relationship between surface temperature and apparent strain is dependent upon endhouse thermal insulation. They have furthur shown that the sense of both the yearly cycle and that of the man induced heat transients following maintenance are the same for a particular micrometer orientation, whereas the sense of the diurnal variation (tidal and temperature variations) is not dependent upon mechanical orientation. The Nevada data corroborates the Aleutian findings and exhibits amplitudes of 3- to 7-thousand micro-inches in response to temperature amplitudes of 30°F while the Aleutian cycles are of order 1- to 2-thousand micro-inches for temperature amplitudes of 10°F.

The most salient features of these cyclic phenomena are that they are largely instrumental "apparent" strains and that they are neither necessarily symmetric nor of the same size or shape for instruments buried in the same vault. Removal of this noise, unique to each instrument, will generally necessitate data strings several years in extent. If it is assumed, however, that long term temperature cycles contain no appreciable contributions from constituents of periods greater than one year, that is, if any temperature induced "apparent" strains will be removed by examining a one year difference, then one year of data is sufficient. This assumption is made in the analysis of the Nevada data.

Also notable on the yearly plots is the anepisodic nature of the strains. Whereas records from the Aleutian Islands frequently show variations of up to 1.0×10^{-6} in time spans of hours to days (Major, 1971), the Nevada records, where continuous, can be characterised as being singularly free of such episodic events.

The Aleutian episodes are suspected to have a relationship to precipitation. In this light it is of interest to examine the precipitation data from the Yucca weather station (Fig. 11, YBO) and to note that in the "wet" February and March of 1970, the components with continuous

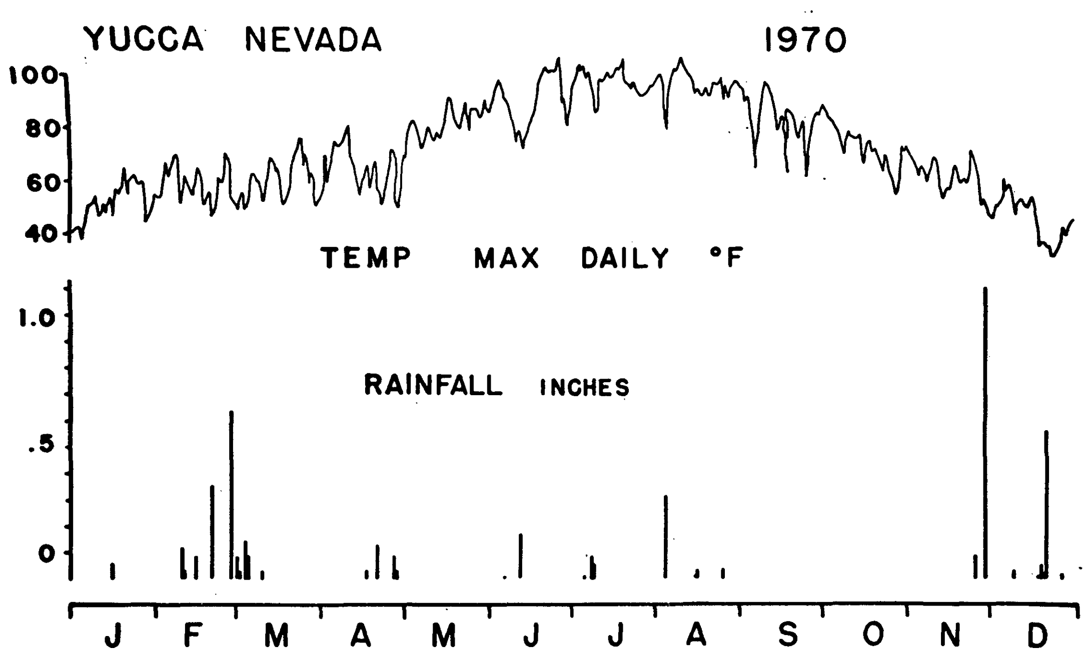

Figure 11. Weather data plot YBO: Yucca, Nevada.

records do not exhibit unusual activity. Even with a scarcity of continuous data, episodes of the Aleutian type are conspicuous by their absence.

II INTERPRETATION

Though limitations upon data handling are imposed by the length of the data string, the large sample interval of much of the data, and a spurious seasonal signal unique to each instrument, the data exhibit evidence of secular trends.

Thirsty Canyon

Upon examination of the TRC curves, Fig. 8, it would seem that estimates of secular drift would be pointless since the cycles suggested by the little more than half a year of data seem quite different. Note that the time span from January to April 1970 has been disregarded as a site curing effect. Indeed, the apparent areal strains in Figure NW + NS and EW + NS, are grossly dissimilar, yet because the micrometer orientation of the NE instrument is opposite that of the others, it is possible, upon assuming that the temperature cycle in each instrument is identical, to make rough estimates of secular drift.

As mentioned in the previous section, reversal of micrometer direction also reverses the polarity of the yearly cycle, so that assuming identical seasonal cycles, the NE + NW areal strain curve (Fig. 12) represents a "true" areal strain by cancellation of temperature effects. Examining the April to late August portions of these record, (arrow on Fig. 12), we have

$$\epsilon_{NW} = e_{NW} + T, \quad \epsilon_{NE} = e_{NE} - T, \text{ where}$$

ϵ = apparent strain

e = true strain

T = thermal effect

$$\epsilon_{NW} + \epsilon_{NE} = e_{NW} + e_{NE} = \text{AREAL STRAIN} \approx 0$$

If it is assumed that the areal strains are equal, then

$$e_{NS} + e_{EW} \approx 0$$

so

$$\epsilon_{NS} + \epsilon_{EW} = e_{NS} + e_{EW} + 2T \approx 2T \approx -3.4 \times 10^{-5}$$

from Fig. 12. Therefore for the portion of the records under consideration, $T \approx -1.7 \times 10^{-5}$, and from Fig. 8 it is seen that $e_{NW} \approx e_{NE} \approx 0$ and $e_{NS} \approx -3.4 \times 10^{-5}$ and $e_{EW} \approx 3.2 \times 10^{-5}$. The earth strain uncontaminated by temperature effects reduces to essentially NS and EW principal axes with NS compression and EW extension. The strain rates indicated are abnormally high, almost 1.0×10^{-4} per year. However Smith and Kind (1972) have interpreted similar strain data from this area as containing large "episodic" strain changes. Therefore extrapolation of these strain rates to longer periods of time might be unwarranted. Perhaps only

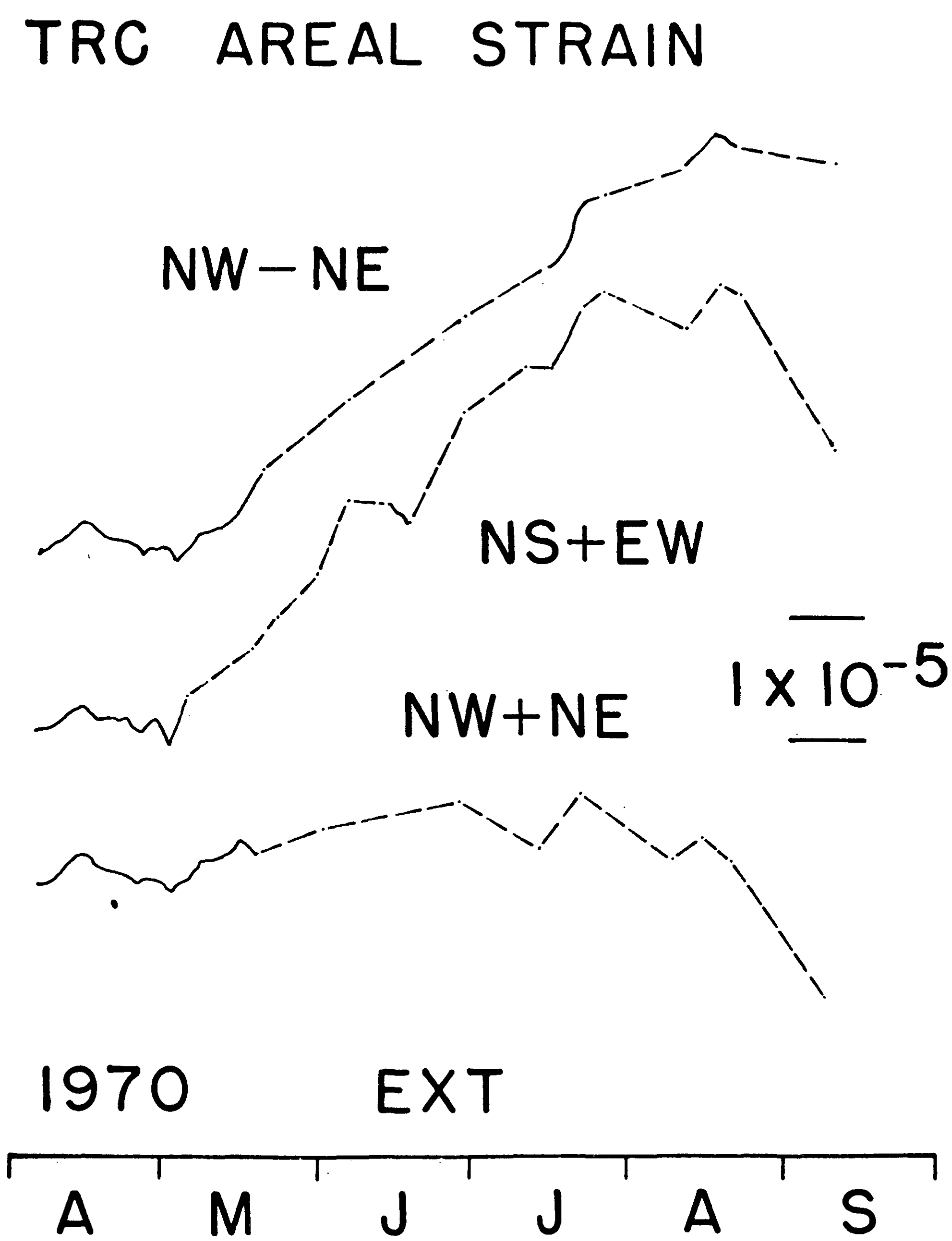

Figure 12. TRC areal strain plot: Rock compression up.

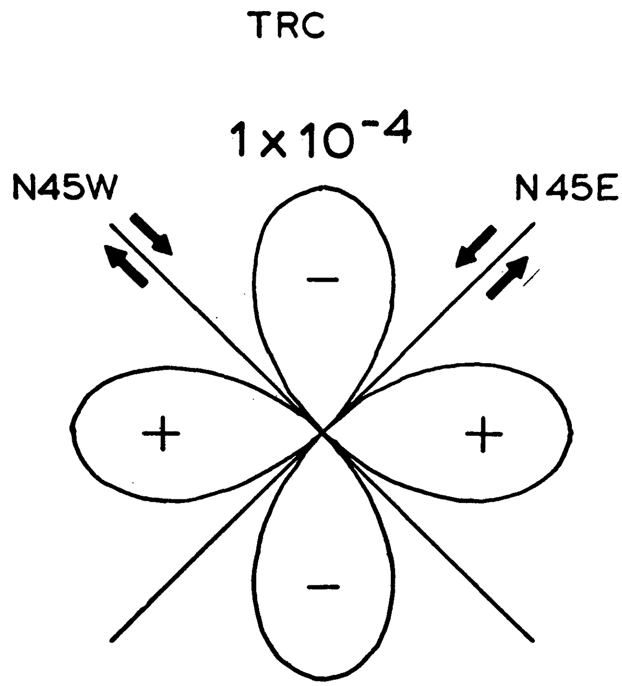

Figure 13. TRC secular strain lemniscate.

the directions of the maximum shear are salvageable with any degree of assurance. The resulting strain figure is shown in Fig. 13. As is evident, the planes and senses of maximum shear stress are N45E, left-lateral, and N45W, right-lateral.

Although the check on internal consistency has been eliminated by the assumption that the areal strains were equal, redundancy combined with the fortuitous reversal of transducer orientation has permitted the extraction of useful results where otherwise it would have been impossible. For a graphical corroboration of the assumptions, note the NW - NE curve which should equal 2T under our assumptions. The curve fits remarkably well with the EW + NS curve which under our scheme should also equal 2T.

Sleeping Mountain

The SPM data (Fig. 9) exhibit non-symmetrical cycles of different amplitude for each component. The fact that each instrument is buried in a separate vault with varying thicknesses of cover might well explain these effects. The reduction of the data is routine because no redundant measurements are involved and the data string is longer than a year. The June 1970 to June 1971 differences are:

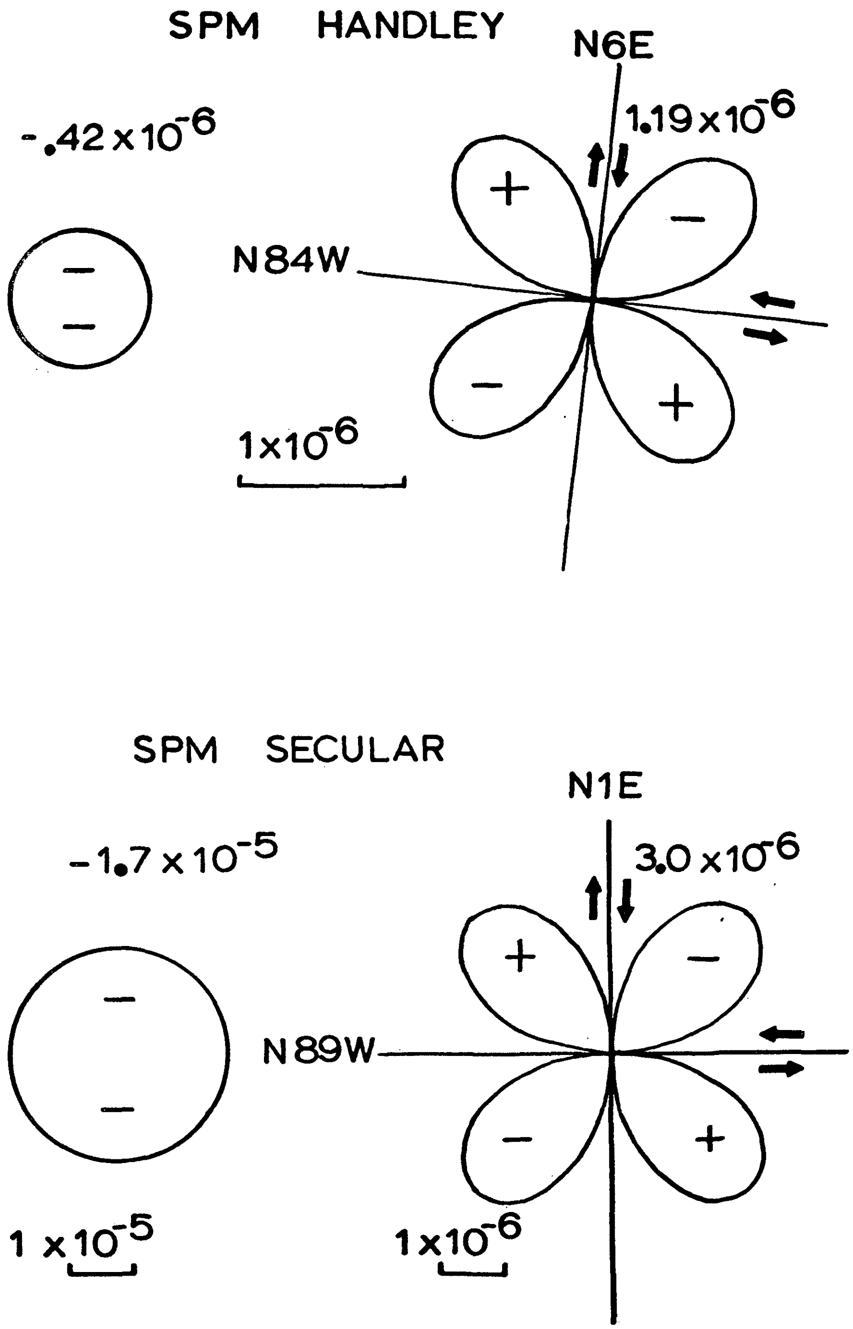

Figure 14. SPM areal and deviatoric strain for both Handley and secular measurements.

$$e_{NS} = -1.4 \times 10^{-5}$$

$$e_{EW} = -2.0 \times 10^{-5}$$

$$e_{NW} = -0.7 \times 10^{-5}$$

The resultant strain, Fig. 14 , indicates compression in all directions and a net areal strain of -3.4×10^{-5}. The maximum principal compression is directed N46E, of magnitude, -2.8×10^{-5}, and the minimum principal compression is directed N44W, of magnitude, $-.5 \times 10^{-5}$. The planes and senses of maximum shear strain are N01E, right lateral, and N89W, left-lateral.

SCOTTY'S JUNCTION

The SCT data string (Fig. 10) is over 15 months long and strongly exhibits yearly cycles on all components. The time period from mid-March to mid-May 1970 has been discarded as a site curing effect. The NW component, the trace of which shows the largest amplitude cycle, contained a section of aluminum tubing until 5 June, 1970, (the first solid arrow on Fig. 10). On that date the instrument was uncovered, quartz inserted into it, and then, reburied. It is suspected that the steep strain rate exhibited from 5 June to late July and perhaps furthur, is may be contaminated by the effects of reburial. The differences in amplitude and phase of the cyclic portions of the vertical strain and the horizontal strain are attributed to differing thermal regiemes since the Z component is buried in a separate, doubly insulated endhouse with the tube in a hole 25 feet deep.

The strain changes from June 1970 to June 1971 as initially determined from these plots are,

$$e_{NS} = +9.0 \times 10^{-6} \qquad e_{NE} = +5.0 \times 10^{-6}$$

$$e_{EW} = +14.0 \times 10^{-6} \qquad e_{NW} = +1.4 \times 10^{-6}$$

$$e_{NS} + e_{EW} = +23.0 \times 10^{-6} \quad e_{NE} + e_{NW} = +6.4 \times 10^{-6}$$

$$e_{zz} = +5.0 \times 10^{-6}$$

As is apparent, the areal strain changes, the sums of orthogonal horizontal components, differ considerably in size, though their signs are the same. Making a least square fit to such inconsistent data would be useless and computing strain lemniscates computed from groups of three components would result in differences in sense as well as magnitude.

The only horizontal component whose testimony we have any reason to impeach is the NW; in particular, that portion of the record displaying the unusually high strain rate immediately following reburial (indicated in Fig. 10 as the trace between the two solid arrows). Soil compaction in the fill and changes in the thermal regime might both contribute to the effect. The thick broken line in Fig. 10 represents the NW trace extrapolated backward from what seems to be a more well behaved portion of the record. The strain change resulting from this projection is 1.0×10^{-5}, so that the yearly strain difference for the NW instrument becomes 11.0×10^{-6}. This brings the areal strains up to the same order of magnitude, but since the full extent of what has been interpreted as anomalous in the NW trace is not known, the strain lemniscate is computed without the NW component.

The strain lemniscate divided into areal and deviatoric strain are plotted in Fig. 15. The figures indicate a net areal extension, the maximum principal extension N60W, 1.8×10^{-5}, and the minimum principal extension, N30E, 4.5×10^{-6}, with the directions and senses of maximun shearing strain N15W, right-lateral and N75E, left-lateral.

Areal strain is plotted from the time of reburial for one year in Fig. 16. Also plotted is -.84 times the vertical strain, Z, corresponding to the theoretical areal strain for a Poisson's ratio of .45 at a stress-free surface. The three curves should coincide, yet as is obvious, the differences are substantial. Several inflec-

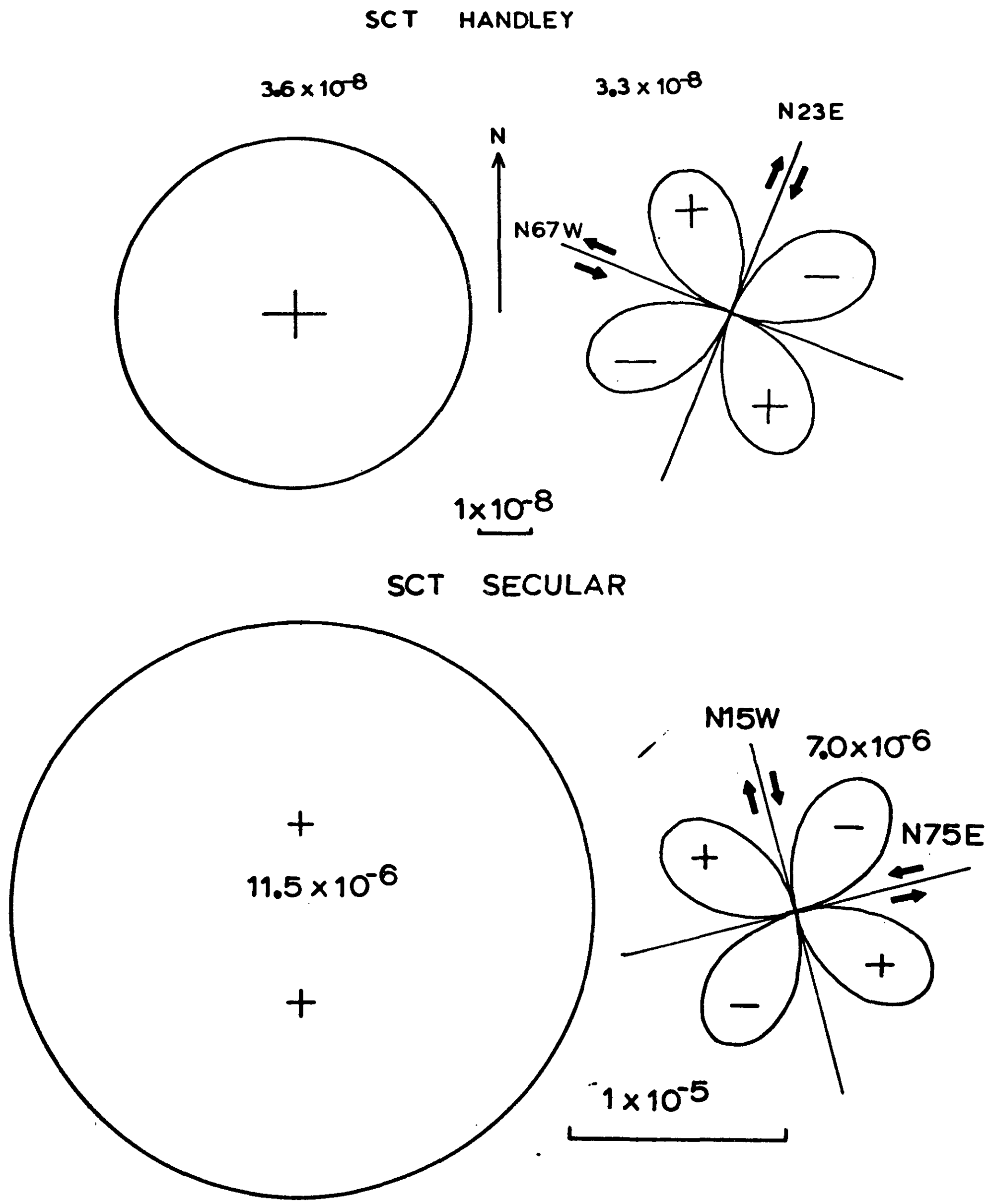

Figure 15. SCT areal and deviatoric strain for both Handley and secular measurements.

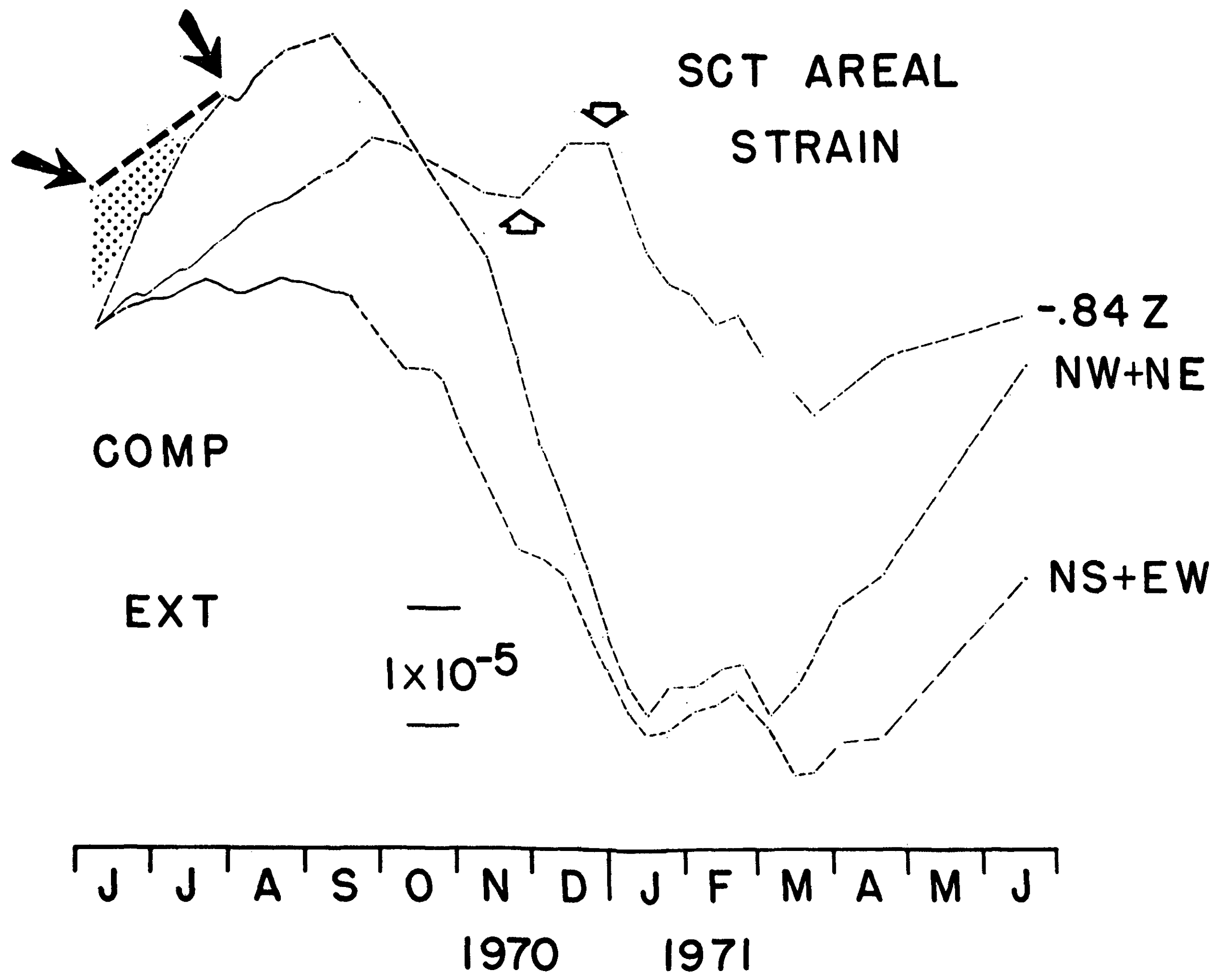

Figure 16. SCT areal strain plots: Rock compression up.

tions during the period from January to March, 1971, are reflected in all three traces and the general shapes of the two horizontally measured areal strain curves are similar to each other. The principal difference between the two seems to originate from the first several months of data from the NW instrument which causes a very high strain rate in the NW + NE areal strain during the same period (indicated in Fig. 16 by the two solid arrows). The thick broken line in Fig. 16 represents this portion of the trace as it would appear if we use the extrapolated NW trace of Fig. 10. As can be seen the difference in directly measured areal strain is reduced to 7.0×10^{-6}, still substantial but much more satisfying than the other one.

The second problem is to reconcile the net yearly vertical strain change with those of the horizontals, for, as is evident, the vertical strain trends in the same sense as the accepted areal strain. The areal strain determined by the vertical strain, $-.84Z$, shows a slight compression of 1.0×10^{-6} while the horizontal areal strain is definitely an extension of several parts in 10^{-5}. As was shown in eqns. 21, the vertical strain at a free surface should be in the sense opposite that of the areal strain, so that multiplication of the vertical strain by $-\lambda/(\lambda+2\mu)$ should then make the resulting measure of aeal strain, in this case -0.84Z, of the same sign as the horizontally measured areal strain. As is evident, direct calculation from these data would result in a negative Poisson's ratio. The physical unacceptability of such bizzare behavior necessitates re-examination of Fig. 10. The most curious feature of the Z trace is the anomalous 25 November to late December portion (denoted by hollow arrows in Figs. 10 and 16) which is not reflected in any of the other traces. Though the records themselves do not give any indication of a polarity reversal, the very presence of such a steep change in slope during a period of relatively smooth variation of the other components compels one to assume the possibility of an instrumental problem. Hypothesizing a polarity reversal for this interval, and using the NS + EW areal strain as the most reliable, the Poisson's ratio will become positive, but still less than 0.2. This is much more satisfying, but since a Poisson's ratio of 0.45 was measured for the Handley test, it may indicate substantial differences in earth response to deformations of different temporal extent.

In order to achieve an acceptable degree of internal consistency, we have been compelled to challenge a combined total of approximately 4 instrument-months of data, from the NW and Z traces. Smith and Kind (1972) with a network of single component sites with station separations comparable to our own, have discarded entirely the record of one of their sites while determining a regional strain field for southern Nevada. While it is regretable that our data is not faultless, we nonetheless consider it to be the best strain data yet obtained for the region.

DISCUSSION

In this paper two classes of redundancy have been discussed; redundancy of instrumentation at a point (SCT), and redundancy in the form of a multiplicity of observatories in the same area. Redundancy of instrumentation at a point has permitted testing the internal consistency of both the Handley steps and the secular data by the computation of both the Poisson's ratio and independent measures of areal strain. Redundancy in the form of a multiplicity of stations in the same area will permit the testing of the homogeneity of the "regional" strain field. Finally, a third possible redundancy may arise from measuring both strain steps and secular strains. First, however, we arrive at some tentative conclusions concerning strain rates and Poisson's ratio calculated from the secular data.

Since the average secular strain rates observed in southern Nevada, 1.0×10^{-4} per year (extrapolated from 4 months) at TRC, and 2.0×10^{-5} per year at both SCT and SPM, are reflected on many instruments, some with separate pier systems, it is unlikely that these strain rates are vagaries of floating or sliding piers. We consider them to reflect real ground deformation. The large magnitude of the observed secular strain rates, if extrapolated over several years, indicate that were the deformation purely elastic, the rocks at each site would rupture in time spans of 1 to 5 years. In view of interpretations which suggest that episodic strain events compensate for large strain rates, .5 to 1.0 x 10^{-5} per 6 months (Smith and Kind, 1972), perhaps such extrapolation is unwarranted. Rates on the order of 3.0 x 10^{-5} per year have been observed and interpreted as tectonic in origin by Romig (1969) in northeast Denver. The majority of reported secular strain rates, however, are an order of magnitude less than ours; 2.0 x 10^{-6} per year in a vault at Granite Mt., Utah, (Anderson, 1972); 2.0 x 10^{-6} per year in a mineshaft at Round Mt., Nevada, (Malone, 1972); and less than 3.0 x 10^{-6} per year in the seismically active Aleutian Islands, (Butler and Brown, 1972). In view of the great variability of the areal strains here observed, 0.0 x 10^{-5} at TRC, 2.3 x 10^{-5} at SCT, and -3.4 x 10^{-5} at SPM, it is reasonable to consider them as site related, small scale (up to a few kilometers in extent) phenomena. From the large size and limited geographical extent of these areal strains, we can hypothesize that the deformation is not purely elastic, that is, perhaps the measurements contain substantial inelastic portions resulting from near-surface, soil creep during the year.

Readdressing the secular measure of Poisson's ratio, at best, positive and less than .2, it is found that the ground at SCT would have to behave quite differently to long term deformation than to short term phenomena such as strain steps, for which a Poisson's ratio of .45 was determined. This situation is unsatisfactory and leads us to search for possible explanations. One such explanation is provided by the hypothesis of the preceeding paragraph, soil creep. Assuming that the creep occurs only in the horizontal plane, that is, that the mechanisms of deformation are different for long term vertical and horizontal observations, or that the point approximation does not apply as well in the vertical dimension for surface creep which decays to insignificance at depths less than the depth of the bottom of the vertical strainmeter, 35 feet, the inconsistency may be explained. The larger the magnitude of $0 < \frac{-e_{33}}{(e_{11}+e_{22})} < 1$ becomes, the greater becomes Poisson's ratio, so that contamination of the horizontal measurements and not the vertical will result in a small Poisson's ratio.

The assumption of horizontal creep will explain both the Poisson's ratio and the size of the strain rates and also fits well with the local, site related character of the areal strains. While it has not been shown to be the case, inelastic deformation is an attractive explanation because it is not unreasonable to expect over the time span of a year.

In discussing secular trends, it is enlightening to compare the relation of the deviatoric portions of the observed secular strains to the microtectonics of the region. Smith and Kind (1972) have published a schematic tectonic map, Fig. 17. The locations and orientation of his strainmeters are indicated by solid bars. Data collected between December 1970 and August 1971 have led them to conclude that the "regional" strain field for this area has principal axes oriented NW and NE, with oscillatory or episodic variations. The three CSM-EML strain observatories are plotted on this map and the planes of maximum shear strain corresponding to each station are plotted in the margin. TRC, the station at which a purely deviatoric strain was deduced, is almost atop an inferred fault. The orientation and sense of slip of this fault matches well with one plane of maximum shear strain of the secular solution. At SCT, the right lateral plane of maximum shear strain corresponds to the azimuth and sense of the local structural trends. At SPM, however, neither of the shear solutions seems to fit as well as those of

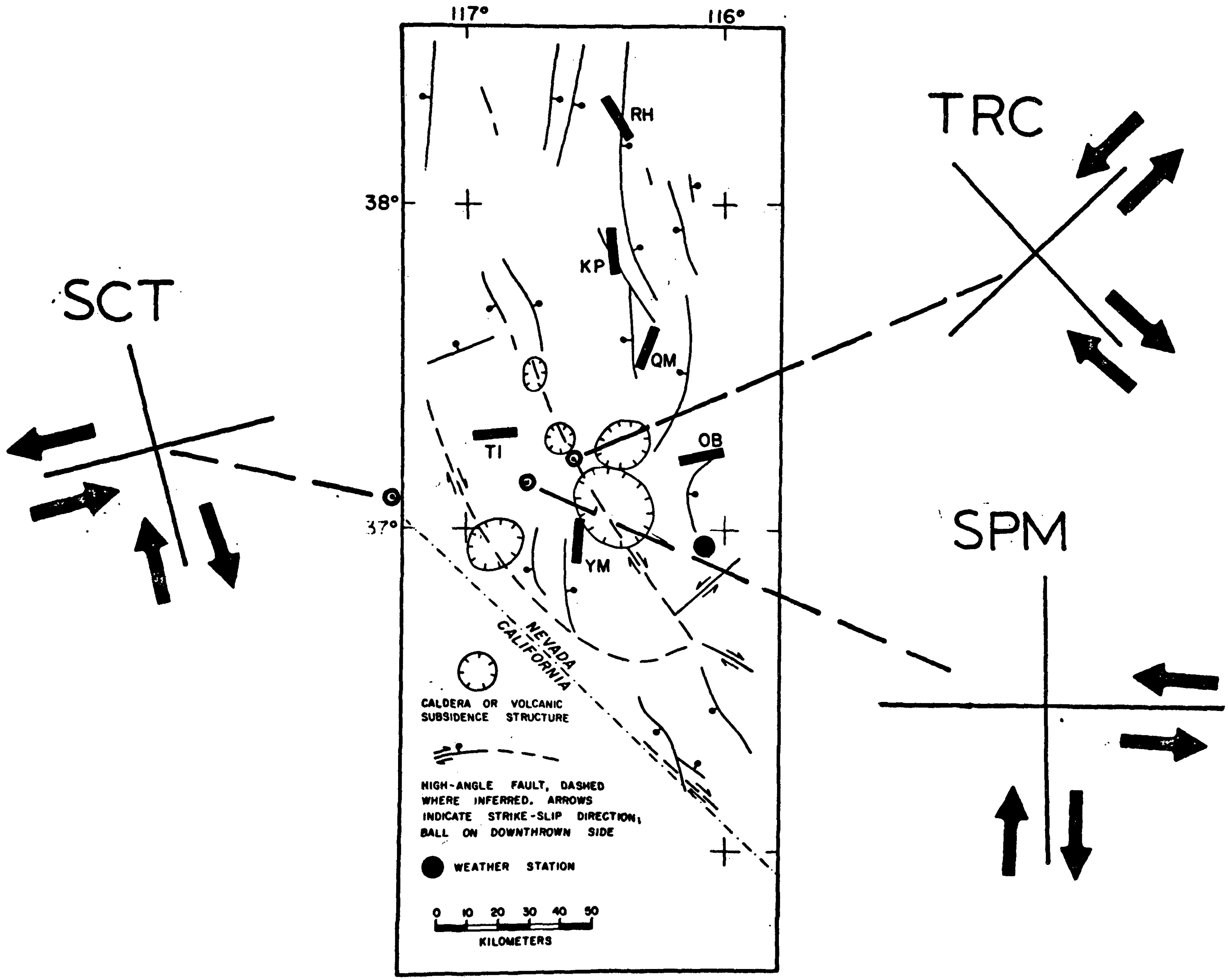

Figure 17. S. Nevada tectonic map (Smith and Kind, 1972).

the other two stations.

Problems remain with this qualitative similarity, yet we conclude that the shear solutions relate fairly well to the structural trends, while the areal strains are highly variable in space, changing from essentially zero to compression, to extension within the distance of 60 to 70 kilometers. It seems that the areal strains are more site specific than the deviatoric strains. This argument, that the shear strains are more reliable than are the areal strains in secular interpretation, has been previously advanced by Romig (1969) in a study of strain data from northeast Denver.

Smith and Kind (1972) have deduced a "regional" strain field from a network of single component stations over a period of 5 to 7 months. The results of the previous discussion of yearly cycles would indicate that, unless instrument thermal insulation is extraordinary, one year of data is the barest minimum necessary to determine secular drifts. Armed now with the results of the present discussion, it is evident that even with three component stations, which permit the separation of deviatoric strains from the highly variable and site specific areal strain, the extraction of "regional" strain is quite difficult. The determination of such regionals from separated single component data contaminated with local areal strains is very hazardous.

A third possible redundancy is suggested by a curious similarity between the step and secular data. Figs. 14 and 15 display the strains at SPM and SCT, respectively, for both the Handley steps and the year long secular strain change. Handley data from TRC was not recoverable so that no similar comparison can be made. The SPM data exhibit a remarkable similarity; both the step and secular strain indicate areal compression, and furthur the orientations and senses of both deviatoric strain figures are almost identical.

The SCT data indicate areal extension for both the shot and the yearly difference, and the diviatoric strains do not seem to correspond to one another. Recall that the Handley strain lemniscate for SCT, Fig. 15, was symmetrical with respect to the source radius. It would seem that the deviatoric portions of the strains observed at SCT, 70km from the source, exhibit the direct effects of the source mechanism. The deviatoric portions of the SPM Handley steps, however, 27km from the source (azimuth to Handley N50E), may be related to the observed secular strains just as easily as to the Handley source. The areal strains at both sites seem to be related to the secular strains at each site, and therefore to the local tectonics as well.

We are led to hypothesize that perhaps, at some locations, the resultant strain steps are as closely related to the fact that the local pre-stressed medium was shaken, as to the precise manner in which the shaking was applied. This hypothesis offers possible explanation of the difficulties encountered in attempting to relate strain seeps observed at different locations to one source mechanism.

Boucher et al (1971) have proposed that Handley strain steps observed at Round Mt., Nevada, are characteristic of the release of pre-existing strain energy; that is, the disturbance of a pre-stressed medium resulted in a jump to a lower energy configuration, the energy having been expended in the strain steps. The steps must be in the opposite sense to the tectonic strain previouly accumulated, that is, a relaxation toward the unstressed configuration. This argument would indicate that secular strains observed in southern Nevada are in the sense of energy release rather than accumulation. Alternatively, one may prefer to believe that the long term strain change is in the sense of departure from equilibrium or elastic energy accumulation, then so too are the strain steps. In this latter case, however, it is difficult to visualize a mechanism to relate the senses and sizes of the one to the other. As it is impossible to determine which is the case, the question is abandoned and we turn to speculate on a model mechanism which would produce strain steps similar to the observations.

Perfect elasticity for long term strains seems to be a tenuous assumption, and instrumental hysteresis has been discounted by the consistency of the SCT Handley steps, but hysteresis of the ground has not yet been considered. White (1969) has proposed a non-linear earth model with an attenuation mechanism based on Coulomb friction in a granular material. A schematic representation of the model consists of a spring-mass system with friction for relative motion between adjacent masses, Fig. 18. The resulting non-linear stress-strain relationship displays hysteresis as shown in Fig. 19. Beginning at a zero stress, zero strain position and applying increasing stress, the strain follows the line of slope $K(1+\gamma)$. Having reached a maximum, as the stress is decreased, the strain will remain constant until the elastic line, slope K, is reached, and then will decrease along a line of slope $K(1 +\gamma)$. Subsequent reversals of stress must be along lines of slope $K(1 +\gamma)$ but maxima and minima must be joined to the elastic line by vertical segments of stress change with no

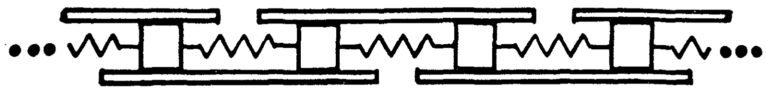

Figure 18. Schematic diagram of internal friction loss mechanism.

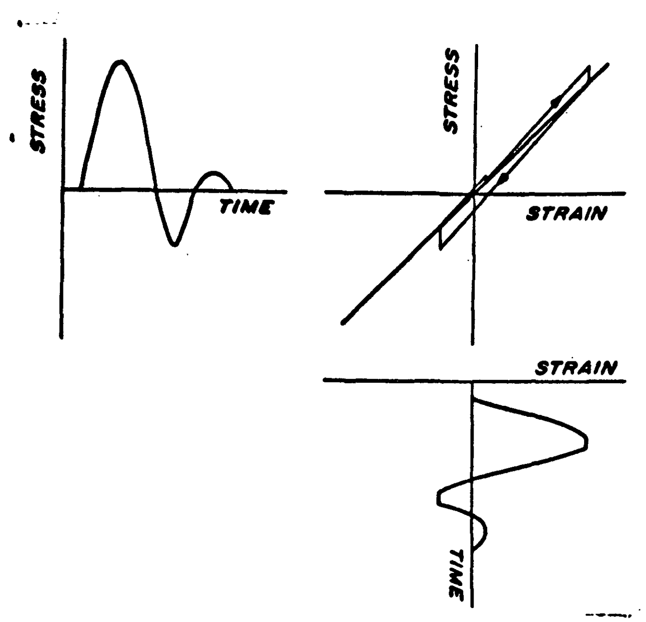

Figure 19. Hysteresis of a White solid (White, 1969a)

strain change, representing the build-up of stress to overcome static friction.

The intriguing characteristic of the model, as pointed out by White (1969), is that if the material is pre-stressed in a monatonic fashion to a static level, the introduction of a small amplitude transient will result in a strain step. It is notable that the direction of the strain step is in the same sense as the pre-strain and the magnitude of the step, $\gamma \epsilon_i$ is proportional to the initial pre-strain ϵ_i. The minimum stress transient necessary to produce a step is $K\gamma\epsilon_i$. Fig. 20 illustrates the phenomenon and Fig. 21 illustrates a computed strain record. Fig. 22 indicates computed strain steps resulting from introducing a transient to the model with a time varying pre-stress, the M_2 earth tidal component. This case demonstrates that the size of the step is proportional to the monotonically increasing (decreasing) strain change since the last reversal in sense, while the sense of the step is always in the direction of the increasing (decreasing) ambient pre-strain. The stored energy may thus be increased or decreased, depending upon the strain history. Also to be noted is that the step change will decay away when the sense of pre-strain is reversed.

Generalizing from a bar to a semi-infinite, isotropic

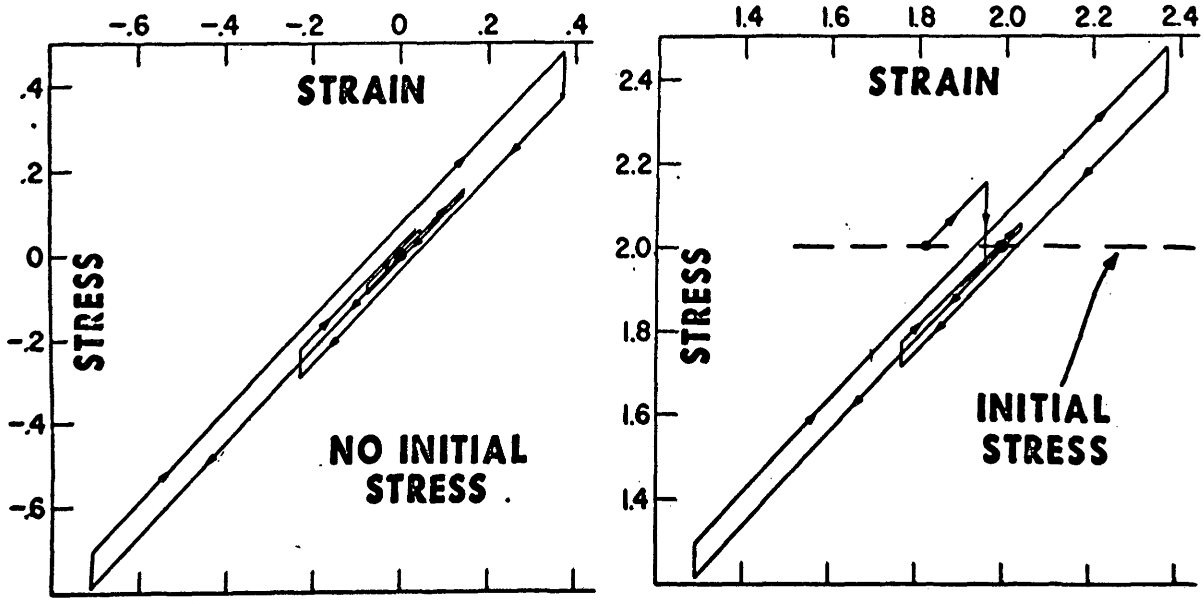

Figure 20. Stress-strain for a transient with pre-stress and without (White, 1969a)

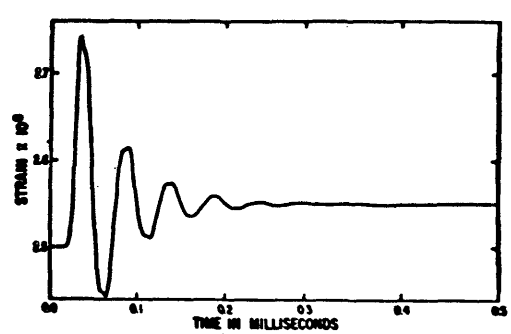

Figure 21. A computed strain step resulting from a transient imposed on an initially stressed White solid (White, 1969b)

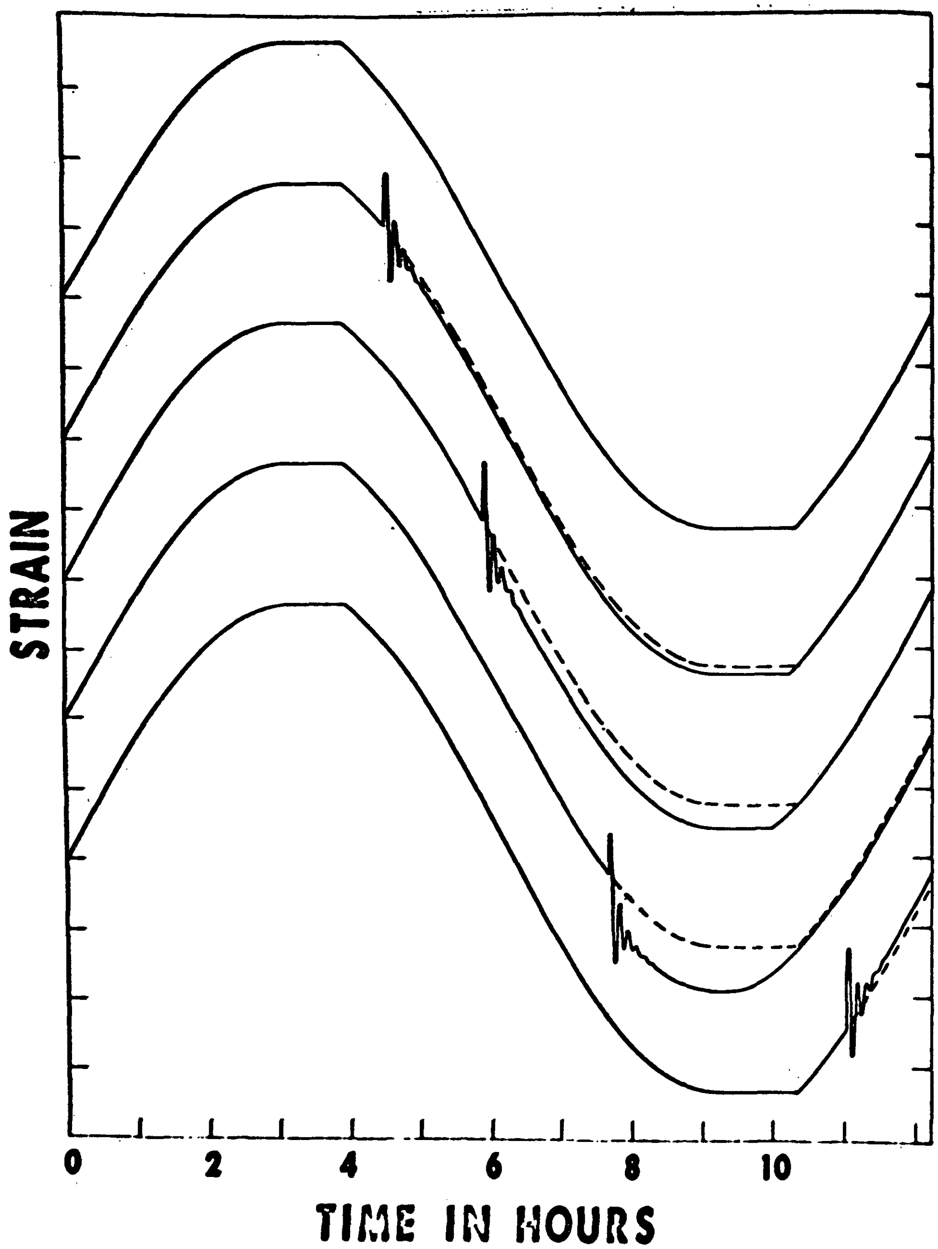

Figure 22. Strain steps with the earth tide as the ambient stress (White, 1969a).

medium will require two constants, but the principle remains the same. Only the constant of proportionality becomes more involved for the pre-strain-step relationship. An isotropic White solid pre-stressed in a monotonic manner will give a strain step ellipse identical to the pre-strain ellipse if disturbed by a transient.

It must be commented that this mechanism is not proposed for all strain steps. Wideman and Major (1967) have shown a distance vs. strain step amplitude relationship, and an earthquake Magnitude-distance-step amplitude relationship. Such relationships are not to be expected for the mechanism proposed. In view of the minimum amplitude necessary for the stress transient to induce a step, proportional to the pre-strain, the far field should be free of such steps. It is hypothesized that in the near field, both the non-linear mechanism and the standard dislocation theory mechanism are involved, and as demonstrated by SCT and SPM there is no consistent predictability. In such cases, strain steps may occur in unpredicted configurations at azimuths unpredicted by source mechanism models, and source related strain steps may be contaminated by non-linear steps.

CONCLUSIONS

The results of this research indicate that:

(1) Redundant observations of strain steps at SCT, 70km from the Handley source, indicate no significant deviation from ideal elastic behavior; deviations are within the error of the measurements, and the Poisson's ratio, .45, is of the order of independent estimates.

(2)a Redundant measurements of secular strain at SCT yield areal strains which differ by a factor of 1/3 and a Poisson's ratio of less than .2.

(2)b The large secular strain rates, 2.0×10^{-5} per year, and the small Poisson's ratio can be explained by the assumption that yearly strain differences contain substantial contributions from inelastic, near-surface soil creep.

(3)a Secular areal strains are highly variable within distances of 70km.

(3)b Secular deviatoric strains correspond to local tectonic trends, but local in the sense of areas about 25km in extent.

(4)a Because of large amplitude seasonal cycles and the site related character of the areal strain, 3 component stations with at least a year of data are necessary for determinations of secular drift from trenched, surface strainmeter data.

(4)b Even with the necessary conditions, estimates of "regional" strain fields are difficult because of the apparent influence of local tectonics.

(5)a At SPM and SCT the areal strains resulting from the Handley test are in the same sense as the secular areal strains. Since SCT is extension and SPM in compression, they seem to relate more closely to local tectonics than to the same source.

(5)b At SCT the deviatoric portion of the Handley strain steps does not resemble the secular deviatoric strain and seems more closely related to the shot source.

(5)c At SPM the Handley deviatoric strains seem to relate as well to the secular deviatoric trends as to the source.

(6)a It is possible that local pre-stresses can influence strain steps as much as do the particulars of a source.

(6)b The non-linear earth model of White (1969) is an attractive mechanism for relating strain steps, and tectonic pre-stresses.

BIBLIOGRAPHY

Anderson, Jerry M., 1972, A study of the possible correlation of strain, tilt, and earthquakes: Univ. of Utah Master's Thesis.

Benioff, Hugo, 1935, A linear strain seismograph: Seism. Soc. America Bull., v. 22, p. 283-309.

__________, 1959, A fused-quartz extensometer for secular, tidal and seismic strains: Geol. Soc. America Bull., v. 70, p. 1019-32.

Berger, Jon, 1972, A year of strain observations in southern California: paper presented at the annual Earthquake Research Review Conference, Boulder, Colo., July 26-28.

Birch, Francis, ed., 1942, Handbook of physical constants: Geol. Soc. America Spec. Paper 36, p. 86.

Boucher, G., Malone, S., and Homuth, E., 1971, Strain effects of nuclear explosions in Nevada: Seism. Soc. America Bull., v. 61, no. 1, p. 55-64.

Brown, Paul L., 1972, Pinon Flat: North/South strain from April 28, 1972 to July 7, 1972: paper presented at the annual Earthquake Research Review Conference, Boulder, Colo., July 26-28.

__________, 1973, Colo. Sch. of Mines Thesis, in prep.

Butler, David, and Brown Paul, 1972, Secular strain measurements before and after the Cannikin nuclear test: Seism. Soc. America Bull., v. 62, no. 6, p. 1455-58.

Cook, Kenneth, 1972, Correlation of earthquakes with changes in strain and tilt near the Wasatch fault, Utah: Abstract Sixty-seventh Seism. Soc. America Meeting, March 30- April 1, Honolulu, Hawaii.

Major, M.W., 1971, Strain episodes in the Aleutian Islands: Abstract Sixty-sixth Seism. Soc. America Meeting, March 25-27, Riverside, Calif.

Major, M.W., Sutton, G.H., Oliver, J., and Metsger, R., 1964, On elastic strain of the earth in the period range 5 seconds to 100 hours: Seism. Soc. America Bull., v. 54, no. 1, p. 295-346.

Malone, Stephen D., 1972, Earth strain measurements in Nevada and possible effect on seismicity due to solid earth tides: Univ. Nevada Ph.D. dissertation.

Murdock, J., 1971, Nevada strain data--acquisition, data reduction, and preliminary analysis: Earthquake Mechanisms Lab., NOAA Progress Report.

Press, Frank, 1965, Displacements, strains and tilts at teleseismic distances: Jour. Geophys. Res., v. 70, no. 10, p. 2395-412.

Press, Frank, and Archambeau, C., 1962, Release of tectonic strain by underground nuclear explosions: Jour. Geophys. Res., v. 67, p. 337-343.

Romig, P.R., 1967, A millimicron displacement transducer with mechanical calibration: Colorado School of Mines Graduate Thesis T-1123.

__________, 1969, Secular strain in N.E. Denver, 1968: Colorado School of Mines Graduate Thesis T 1268.

Ryall, Alan, 1972, Small earthquakes in the Nevada region, and earthquake activity and strain changes associated with underground explosions: Tech. Report No. 1, Seism. Lab., Mackay Sch. Of Mines, Reno, Nevada.

Sokolnikoff, I.S., 1956, Mathematical theory of elasticity: New York, McGraw-Hill Book Co., Inc., 2nd Ed.

Smith, Stewart W., and Kind, Rainer, 1972, Observations of regional strain variations: Jour. Geophys. Res., v. 77, no. 26, p. 4976-80.

White, J.E., 1965, Seismic waves: New York, McGraw-Hill Book Co., Inc.

__________, 1969a, Strains in a constant Q solid: Proc. International Congress on Acoustics, Tokyo, 1969.

__________, 1969b, Computed waves in a non-linear solid: In honor of Philip M. Morse, M.I.T. Press, Cambridge, Mass.

White, J.E., and Sengbush, R.L., 1953, Velocity measurements in near-surface formations, Geophysics, v. 18, no. 1, p. 54-69.

Wideman, C.J., 1973, Colo. Sch. of Mines Graduate Thesis, in prep.

Wideman, C.J., and Major, M.W., 1967, Strain steps associated with earthquakes: Seism. Soc. America Bull., v. 57, p. 1429-44.

Yacoub, Nazieh K., Scott, James H., and McKeown, F.A., 1970, Computer ray tracing through complex geological models for ground motion studies: Geophysics, v. 35, no. 4, p. 568-602.

Yeatts, Richard F., 1973, A multipole representation of earthquake source mechanisms: Seism. Soc. America Bull., v. 63, no.1, p. 211-26.